SIAM J. APPL. MATH.
Vol. 60, No. 4, pp. 1270–1301

ON A MODEL OF THE DYNAMICS OF LIQUID/VAPOR PHASE TRANSITIONS*

HAITAO FAN†

Abstract. A model for the liquid/vapor phase transitions in a shock tube is studied. Mathematical analysis for the one-dimensional isothermal case is carried out. A sufficient condition for the existence of traveling waves is given. These traveling waves represent liquefaction and evaporation shocks. The nonexistence of some of these traveling waves when the shock speed is smaller than some number is proved. Major one-dimensional wave patterns observed in actual experiments with retrograde fluids are also observed in solutions of Riemann problems. A rough estimate of the difference of the calculated pressure in the solution of the Riemann problem and that in experimental data due to the modeling is given.

Key words. liquid/vapor phase transition, traveling wave, Riemann problem

AMS subject classifications. 35K57, 35L65, 35L67, 35O30, 76N10, 76T05

PII. S0036139998343204

1. Introduction.

Consider a pure fluid that exhibits liquid/vapor phase changes. The pressure function $p(\rho, T)$ for such a fluid with fixed temperature below critical temperature has the shape depicted in Figure 1.1, where ρ is the density. The region $\rho < \alpha$ corresponds to vapor, while $\rho > \beta$ corresponds to liquid. The line joining $(m, p(m, T))$ and $(M, p(M, T))$ is called the Maxwell line where two equilibrium phases can coexist. The regions $m < \rho < \alpha$ and $\beta < \rho < M$ are called metastable regions. The spinodal region $\rho \in [\alpha, \beta]$ is a highly unstable region where the fluid, if it can enter this region, will quickly decompose into vapor or liquid or their mixture. Thus, the pressure curve $p(\rho, T)$ in this region cannot, at least for now, be measured.

In this paper, we shall concentrate on the dynamic flows involving liquid/vapor phase transitions of retrograde fluids, i.e., fluids with large heat capacities, in shock tubes. There were numerous experimental and computational studies of dynamics of phase transitions in shock tubes. Works on condensation in expansion waves in shock tubes, using regular fluids with inert carrier gases, were initiated and developed by Wegener et al. [WLe, WLu, WW] and notable contributions were made by Sisilian and Glass [SG], Wu [Wu], and Bauschdorff [Ba]. Many of these papers contained models describing the conservation of mass, momentum, and energy coupled with some complicated droplet growth models that govern the phase changes. These complicated droplet initiation and growth equations tend to be difficult when subjected to mathematical analysis. Experimental and computational studies on phase transitions in shock tubes using retrograde (i.e., with large heat capacity) fluids were carried out by authors of [GTC, TCK, TCMKS], where they observed a number of interesting wave patterns. For details of the definition of retrograde fluids, see [TCMKS].

As shocks or rarefaction waves pass through fluid in the shock tube, phase changes are induced. For example, as a compression shock passes through saturated vapor of retrograde fluid, both pressure and temperature will rise. Due to the large heat capacity, the temperature rise is relatively small and so is the equilibrium pressure

*Received by the editors August 10, 1998; accepted for publication (in revised form) July 2, 1999; published electronically March 23, 2000. This research was supported by NSF grant DMS-9705723.
http://www.siam.org/journals/siap/60-4/34320.html
†Department of Mathematics, Georgetown University, Washington, DC 20057 (fan@math.georgetown.edu).

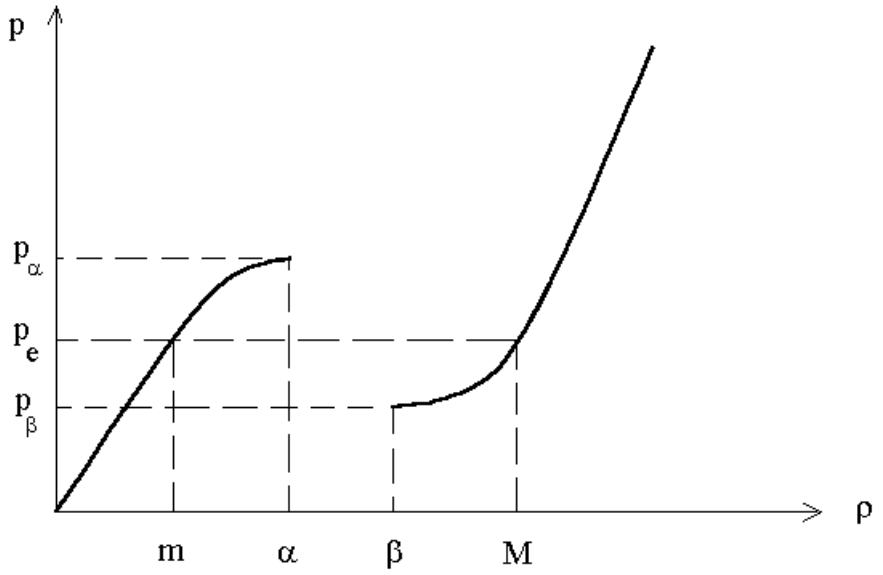

FIG. 1.1.

$p_e = p(m(T), T)$. Then the pressure after the shock is greater than $p_e = p(m(T), T)$ and condensation will occur. Condensation induced by shocks tends to produce fine liquid drops well mixed with the remaining vapor. The passage of the waves is much faster than the process in which these fine liquid drops collide to become large drops. For this reason we shall assume in this paper, for simplicity, that vapor and liquid are always finely mixed. We further assume that the flow is homogeneous. Similar to the systems for multiphase reactive flows, we can derive a model describing such flow in the one-dimensional case as

$$\begin{aligned} &\rho_t + (\rho u)_x = 0, \\ &(\rho u)_t + (\rho u^2 + p(\rho, \lambda, T))_x = \epsilon u_{xx}, \\ &E_t + (\rho u E + up - \epsilon u u_x - \kappa T_x)_x = 0, \\ &(\lambda\rho)_t + (\lambda\rho u)_x = w_1 + \mu\lambda_{xx}, \end{aligned} \tag{1.1}$$

where ρ is the density, u the velocity, T the temperature, E the energy per volume, λ the mass density fraction of vapor in the fluid, p the pressure, and ϵ, κ, and μ are positive constants representing viscosity, heat conduction, and diffusion of vapor in fluid, respectively. The function w_1 is the reaction rate function for vapor phase governing the growth of vapor in the fluid. It typically contains two parts, one for the creation of nuclei of a new phase and the other for the subsequent growth of these nuclei:

$$w_1 = w_{growth} + w_{nucleation}. \tag{1.2}$$

The function w_1 can be very complicated, and there are still several competing theories about these functions; see [KG] and [Sp] for a review on this subject. The modeling of evaporation process is even more complicated; see [Wa]. We shall discuss w_{growth} and the pressure function $p(\rho, \lambda)$ in section 2.

The derivation of (1.1) and (1.2) necessarily involves many assumptions. For system (1.1) and (1.2) to be a valid model for the dynamics of liquid/vapor phase

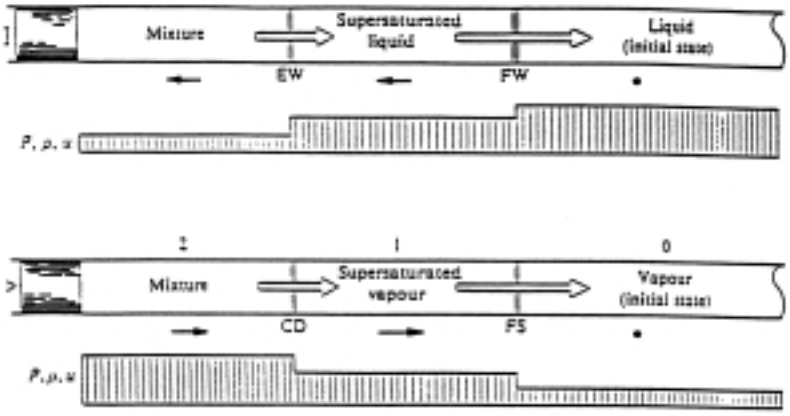

FIG. 1.2. *Conceptual representation of one-dimensional wave splitting in a liquid-vapor system. All waves are traveling to the right. Direction of the impulsive piston motion is indicated by broad-banded arrows, fluid motion by the thin black arrows.* (a) *Rarefaction wave leading to liquid-evaporation splitting. FW = forerunner wave, EW = evaporation wave.* (b) *Compression wave leading to vapor-condensation splitting. FS = forerunner shock, CD = condensation discontinuity.*

transitions, it should at least exhibit wave patterns observed in actual experiments. It would be even better if it offers a hope that qualitative and quantitative agreement between the model and experiments can be achieved by more accurate functions for p and w_1, etc., or by introducing even more variables if necessary.

In this paper, we shall investigate whether system (1.1) and (1.2) can exhibit wave patterns observed in shock tube experiments on retrograde fluids. We shall do so through the study of the traveling waves and solutions of Riemann problems of system (1.1) and (1.2).

We recall major one-dimensional wave patterns observed in shock tube experiments on retrograde fluids summarized in [TCK] and [TCMKS]. The apparatus is a tube with a piston on one side, say the left, and the other side is either open or closed. By compressing or withdrawing the piston, phase transition can be induced. Figure 1.2 is taken from [TCMKS] which summarizes the wave patterns observed when the piston is compressed and withdrawn.

(a) Withdrawing the piston from liquid to send an expansion wave into the liquid. This wave then splits into a forerunner rarefaction wave, which sends the liquid into the metastable region, followed by a slower moving evaporation shock; see Figure 1.2(a). The upstream state of the evaporation shock is overheated liquid.

(b) Compressing the piston into the vapor to send a compression shock into the vapor; see Figure 1.2(b). If the shock strength is not too strong, then this shock will split into a forerunner shock and a slower moving condensation discontinuity across which vapor changes to liquid/vapor mixture or liquid. The slower moving condensation discontinuity is subsonic on both sides of the shock. By further increasing the shock strength, the condensation discontinuity will move faster, and eventually the condensation discontinuity and the forerunner shock merge if the compression strength is strong enough.

When the upstream state is an equilibrium liquid/vapor mixture, then there is no wave splitting.

(c) Withdrawing the piston from the equilibrium liquid/vapor mixture will create a rarefaction shock. The downstream state of the shock is overheated vapor. In fact, given rarefaction initial data, the liquid/vapor system will sharpen up to form a rarefaction shock across which phase transition occurs. This phenomenon was mentioned in [TCK, TCMKS] although no experiment was carried out to demonstrate it.

Much of the mathematical analysis on systems similar to (1.1) has been mostly restricted to the case of premixed ideal gases with Arrhenius-type reactions where the reaction rate functions are typically of the form $w = k\rho\lambda \exp(-E/RT)$, where $k > 0$ and $E > 0$ are constants. These choices of pressure and reaction rate functions are used in combustion in ideal gases. There are few works on (1.1) with other types of pressure functions and rate functions which are suitable for dynamics of phase transitions. Rabie, Fowles, and Fickett [RFF] studied a model of dynamics of phase transitions similar to (1.1), but without the diffusion term in the reaction equation. They used a simple rate law

$$\frac{\partial \lambda}{\partial t} = -\frac{\lambda - \lambda_e}{\gamma}\chi(p \geq p_{ig}), \tag{1.3a}$$

where

$$\lambda_e = \begin{cases} 0 & \text{if } \rho > \beta, \\ \frac{\rho-\alpha}{\beta-\alpha} & \text{if } \beta \geq \rho \geq \alpha, \\ 1 & \text{if } \rho < \alpha \end{cases} \tag{1.3b}$$

and χ is the characteristic function, γ is the typical reaction time, and p_{ig} the ignition pressure. The part $\chi(p \geq p_{ig})$ is a technical assumption to make traveling waves possible when upstream is metastable liquid. They studied the phase plane for the traveling wave equations of (1.1) with (1.3). They also studied the piston problem with initial values in the metastable liquid region. They found a double wave structure in the solutions. However, the choice of the reaction rate equation (1.3), while it is good for studying explosive evaporation, has many limitations: the ignition pressure p_{ig} needs artificial adjustments for different Riemann data. For general initial data, p_{ig} will be difficult to choose. Under the rate law (1.3), metastable states will settle into equilibrium exponentially fast which defies the fact that the metastable state can exist for a relatively long period of time. Also, the rate law precludes the creation of metastable states. The investigation of the effect of nucleation is not possible under (1.3) since no nuclei are required to start the phase change in (1.3). The absence of the diffusion term $\mu\lambda_{xx}$ removes the possibility of moving phase boundary induced by the close neighboring nuclei of another phase.

The dynamics of liquid/vapor phase transitions has also been studied through the investigation of the p-system of conservation laws with the van der Waals type of pressure functions, with which the system is of hyperbolic-elliptic mixed type; see [Sl, Sh, Hs, Fan1]. We shall see that some wave patterns similar to those observed in these studies are also observed in (1.1). However, the system (1.1) is closer to actual experiments; for example, it allows the mixture of liquid and vapor. Moreover, system (1.1), with assumption (1.5) below, is of hyperbolic type which is easier to handle mathematically than hyperbolic-elliptic mixed type systems of conservation laws. The case where the pressure function is that of equilibrium is studied in [MP], which also found the splitting of the shock in the compression case.

Recently, Fan [Fan2] studied the traveling waves and Riemann problems for the isothermal case (i.e., temperature=constant) of (1.1) in Lagrange coordinates:

$$\begin{aligned} v_t - u_x &= 0, \\ u_t + p(v,\lambda)_x &= \epsilon u_{xx}, \\ \lambda_t &= \frac{1}{\gamma} w(v,\lambda) + \mu \lambda_{xx}, \end{aligned} \tag{1.4}$$

where v is the specific volume. Constant temperature can be achieved either when the shock tube is put into a heat bath with very large heat conductivity or when the heat capacity of the fluids goes to infinity. The latter approximates retrograde fluids, whose heat capacities are very large. The pressure $p(v,\lambda)$ is assumed to satisfy

$$p_v < 0, \qquad p_\lambda > 0, \qquad \text{and} \qquad p_{vv} > 0. \tag{1.5}$$

When the right-hand side of (1.4) is 0, the system (1.4) is a strictly hyperbolic system of conservation laws. In the hope of making the system (1.1) mathematically simple enough but still preserving the basic wave patterns of the flow observed in experiments and allowing a fair amount of mathematical analysis as well as exhibiting interesting phenomena, we took

$$w_{growth} = \frac{p_e - p}{\gamma p_e} \lambda(\lambda - 1) \tag{1.6}$$

in [Fan2]. The constant $\gamma > 0$ represents the typical reaction time. More details about our choice of (1.6) are given in section 2.

We note that the $w_{nucleation}$ in (1.2) is not equal to 0 when $p \neq p_e$, which does not allow equilibrium points for traveling wave equations. This is the typical "cold boundary" difficulty. For fluids in the metastable region with pressure not far from equilibrium, it takes some time for these terms to have a sizable effect while the passage of fluid dynamic waves is relatively faster. In other words, the term $w_{nucleation}$ is relatively small in metastable regions. Thus, we took in [Fan2]

$$w_1(\rho,\lambda) = w_{growth} \tag{1.7}$$

in our studies of traveling waves in the isothermal case.

Traveling waves of (1.4) are solutions of

$$\begin{aligned} &-cv' - u' = 0, \\ &-cu' + p' = u'', \\ &-c\lambda' = aw(v,\lambda) + b\lambda'', \\ &(v,u,\lambda)(\pm\infty) = (v_\pm, u_\pm, \lambda_\pm), \quad (v',u',\lambda')(\pm\infty) = (0,0,0), \end{aligned} \tag{1.8}$$

where $a = \epsilon/\gamma$, $b = \mu/\epsilon$, and "$\prime$" denotes $d/d\xi$ with $\xi = (x - ct)/\epsilon$. The system (1.8) can be rewritten as

$$\begin{aligned} &-cv' = c^2(v - v_-) + p - p_-, \\ &-c\lambda' = aw(v,\lambda) + b\lambda'', \\ &(v,\lambda)(\pm\infty) = (v_\pm, \lambda_\pm), \quad (v',\lambda')(\pm\infty) = (0,0). \end{aligned} \tag{1.9}$$

Clearly, the Rankine–Hugoniot condition

$$\begin{aligned} &-c(u_+ - u_-) - (v_+ - v_-) = 0, \\ &-c(v_+ - v_-) + (p_+ - p_-) = 0, \\ &w(v_\pm, \lambda_\pm) = 0, \qquad \lambda_\pm \in [0,1] \end{aligned} \tag{1.10}$$

is necessary for (1.8) and hence (1.9) to have solutions. From above, the speed of a traveling wave is

$$c^2 = -\frac{p_+ - p_-}{v_+ - v_-}. \tag{1.11}$$

In [Fan2], we proved the following results.

THEOREM 1.1. *Assume* $\lambda_\pm = 0$ *or* 1,

$$(v_+ - v_-)(\lambda_+ - \lambda_-) > 0, \tag{1.12a}$$

$$(v_+ - v_-)(p_+ - p_e) \geq 0, \tag{1.12b}$$

and that there is no other equilibrium point of (1.9) *with* v *value between* v_- *and* v_+. *If the speed*

$$c = \sqrt{-\frac{p_+ - p_-}{v_+ - v_-}}$$

satisfies

$$c^2 > 4ab \max(p(v_+, 1) - p_e, p(v_-, 1) - p_e), \tag{1.13}$$

then there is a monotone solution of (1.9). *Furthermore, if* $c^2 < 4ab(p_+ - p_e)$, *then there is no solution of* (1.9) *satisfying* $\lambda \in [0, 1]$.

We note that by the definition of λ, the range of λ must be included in $[0, 1]$ to be physically meaningful. Although Theorem 1.1 is stated for the case $c \geq 0$, it can be easily converted to the case $c < 0$ by a transformation $\xi \mapsto -\xi$ in (1.4), or by interchanging (v_-, λ_-) and (v_+, λ_+) in Theorem 1.1. In [Fan2], we also studied the admissibility of traveling waves and solutions of some Riemann problems. We showed that system (1.4) with (1.5) and (1.7) can exhibit many wave patterns observed in actual experiment on retrograde fluids in shock tubes.

The method for establishing the existence part of Theorem 1.1 is to prove the existence of solutions of a singularly perturbed (1.9)

$$\begin{aligned} &-cv' = c^2(v - v_-) + p - p_- + \eta v'', \\ &-c\lambda' = aw(v, \lambda) + b\lambda'', \\ &(v, \lambda)(\pm\infty) = (v_\pm, \lambda_\pm), \quad (v', \lambda')(\pm\infty) = (0, 0) \end{aligned} \tag{1.9$'$}$$

on finite intervals by using Leray–Schauder degree theory, and then to extend the existence result to $\mathbb{R}$. Finally, we let $\eta \to 0+$ to obtain the existence of solutions of (1.9).

However, the above result on the existence of traveling waves of (1.4) does not cover the important case where the upstream state of a shock is an equilibrium mixture of liquid and vapor. This case is important because many actual experiments involve equilibrium mixture. Also, condition (1.13) is too restrictive. In this paper, we shall improve the earlier result Theorem 1.1 to relax the condition (1.13) and to allow the upstream state of the shock to be an equilibrium mixture.

Our results on the existence of traveling waves are roughly as follows: if the slope of the line connecting $(v_-, p(v_-, \lambda_-))$ and $(v_+, p(v_+, \lambda_+))$ is greater than some number, then there is a solution of (1.9) with speed $c > 0$.

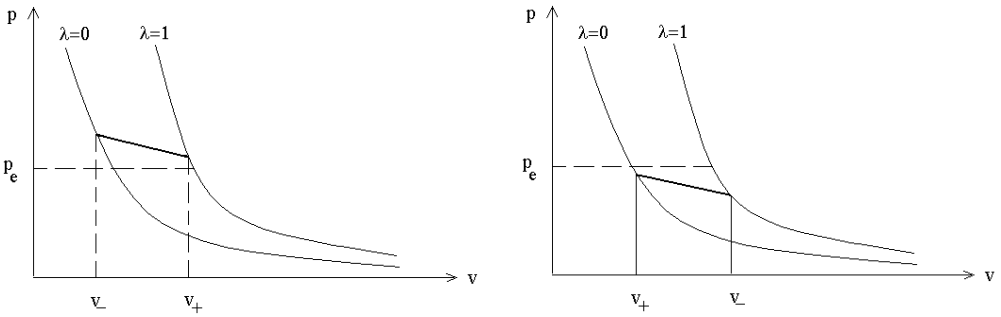

FIG. 1.3.

Precise statements of the main results of this paper are as follows.

THEOREM 1.2. (i) *Assume*

$$(v_+ - v_-)(\lambda_+ - \lambda_-) > 0, \tag{1.14a}$$

$$(v_+ - v_-)(p_+ - p_e) \geq 0, \tag{1.14b}$$

$$c^2 + p_{v\pm} < 0, \tag{1.14c}$$

and that there is no other equilibrium point of (1.9) *with* v *value between* v_- *and* v_+. *If the speed* c *of traveling waves satisfies*

$$c \geq \omega^* := 2\sqrt{ab|p_- - p_e|}, \tag{1.15}$$

then there is a traveling wave solution of (1.9). *If the speed* c *satisfies*

$$c < 2\sqrt{ab|p_+ - p_e|}, \tag{1.16}$$

then there is no traveling wave of (1.9) *satisfying* $\lambda \in [0, 1]$.

(ii) *Assume*

$$(v_+ - v_-)(\lambda_+ - \lambda_-) > 0, \tag{1.14a$'$}$$

$$(v_+ - v_-)(p_- - p_e) \leq 0, \tag{1.14b$'$}$$

$$c^2 + p_{v\pm} < 0, \tag{1.14c$'$}$$

and that there is no other equilibrium point of (1.9) *with* v *value between* v_- *and* v_+. *If*

$$-c \geq \omega^* := 2\sqrt{ab|p_+ - p_e|}, \tag{1.15$'$}$$

then there is a traveling wave solution of (1.9). *If the speed* c *satisfies*

$$-c < 2\sqrt{ab|p_- - p_e|}, \tag{1.16$'$}$$

then there is no traveling wave of (1.9) *satisfying* $\lambda \in [0,1]$.

COROLLARY 1.3. (i) *Let* $\lambda_- = 0$ *or* 1. *For each* (v_-, λ_-), *if* $ab > 0$ *are small enough, then there are* (v_+, λ_+) *such that* $(v_\pm, \lambda_\pm)$ *satisfy* (1.14) *and there are solutions to the traveling wave equation* (1.9) *with speed* $c > 0$ *for such* $(v_\pm, \lambda_\pm)$.

(ii) *Let* $\lambda_+ = 0$ *or* 1. *For each* (v_+, λ_+), *if* $ab > 0$ *are small enough, then there are* (v_-, λ_-) *such that* $(v_\pm, \lambda_\pm)$ *satisfy* (1.14′) *for which there are solutions to the traveling wave equation* (1.9) *with* $c < 0$.

From the above results, we see that the lower bound of the speed of a phase boundary is proportional to $\sqrt{ab}$, where $ab = \mu/\gamma$ is the product of diffusion and typical reaction speed. This confirms the intuition that the faster the reaction speed, the faster the phase boundary moves; and that the larger the diffusion, the more nuclei of one phase are spread into the fluid of another phase and hence the faster the phase transition occurs and hence the faster the phase boundary propagates.

Although some solutions of (1.4) in the $\epsilon \to 0+$ limit found through Rankine–Hugoniot diagrams have been known for years, solutions obtained in this way are nonunique. The result above shows that some of the phase boundaries are not admissible and hence helps in resolving the nonuniqueness. Our method for proving the existence part of Theorem 1.2 is different from what we used in [Fan2]. Here we first modify (1.9) so that it becomes the traveling wave equations for a reaction-diffusion system of partial differential equations. We find that this system is of monotone type. Traveling waves for monotone systems of reaction-diffusion equations are well studied. But our system has an extra complexity: that is, the source term in the reaction-diffusion system also depends on the speed of the traveling wave.

In this paper, we also study Riemann problems which simulate shock tube experiments. We find almost all the one-dimensional wave patterns in shock tube experiments on retrograde fluids listed in [TCK] and [TCMKS] are present in solutions of Riemann problems of the system (1.4). Thus, system (1.4) and hence (1.1) can model pattern of waves of liquid/vapor phase transitions in retrograde fluids in shock tubes. Although we have not carried out a computation based on real data from experiments to access the quantitative agreement between the model and experiments, we will provide a very rough estimate of the order of magnitude of error in this paper. We shall see that if both computation and experiment show a wave pattern as depicted in Figure 1.2(b), the agreement between the calculated pressure and that observed in experiments can be quite good and the accuracy only depends on that of the state functions such as pressure and energy functions, etc.

This paper is divided as follows. In section 2, we recall from [Fan2] some details of the model (1.1), (1.6), and the pressure function. The role of the diffusion term $\mu\lambda_{xx}$ in (1.1) is discussed. In section 3, we prove our main result, Theorem 1.2 and Corollary 1.3. In section 4, we give examples of Riemann problems of (1.4) whose solutions exhibit wave pattern (a)–(c) listed in section 1. A discussion of possible differences of computation and experiments due to the model is given. This suggests that the model can be qualitatively correct at least when calculating the pressure at three points, the right, middle, and left, as depicted in Figure 1.2(b).

2. A model for the dynamics of phase transitions in liquid/vapor systems. We start with the pressure function for the liquid/vapor system. We can observe from experiments the pressure function when the material is in pure vapor phase and liquid phase. Let $p_1(\rho, T)$ and $p_2(\rho, T)$ be the pressure function of pure vapor phase and liquid phase, respectively, where ρ is the density and T the temperature; see Figure 2.1. The Maxwell equilibrium density $m(T)$, $M(T)$ at which

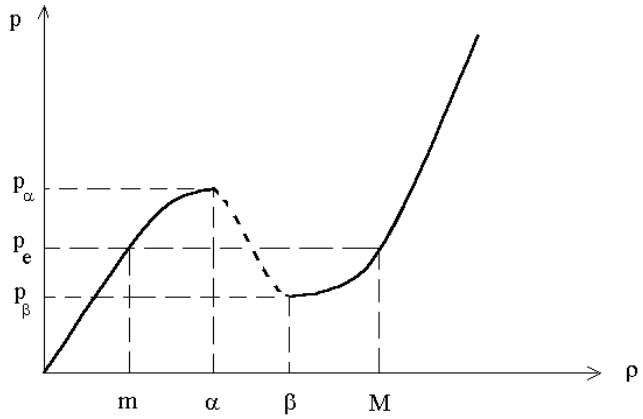

FIG. 2.1.

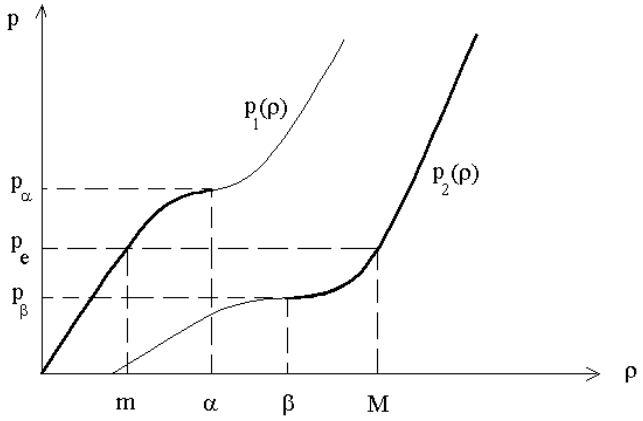

FIG. 2.2.

$p_1(m,T) = p_2(M,T)$ and the liquid and vapor phases can coexist in equilibrium can be measured in the laboratory. The spinodal region $\alpha < \rho < \beta$ is highly unstable where the material instantly decomposes into liquid or vapor or their mixtures. As a result, the portion of the traditional van der Waals pressure curve within the spinodal region, shown as a dashed line in Figure 2.1, cannot be measured in experiments and is probably artificial. Thus, we shall keep only the observable part and proceed without specifying $p(\rho)$ for ρ in the spinodal region. We extend each component of function $p(\rho,T)$ continuously to an increasing function on $\mathbb{R}$, as shown in Figure 2.2, to obtain $p_1(\rho,T)$ and $p_2(\rho,T)$. In other words, the functions $p_1(\rho,T)$ and $p_2(\rho,T)$ are pressure functions for pure vapor and liquid states, respectively. Although the part of these pressure functions beyond the spinodal limit, i.e., $p_1(\rho_1)$ for $\rho_1 > \alpha$ and $p_2(\rho_2)$ for $\rho_2 < \beta$, cannot be measured and our extensions of the pressure functions into the spinodal region are somewhat arbitrary, these parts of the pressure functions do not affect the outcome; for example, the part of the pressure function $p_1(\rho)$ for $\rho > \alpha(T)$ does not have much effect since there will not be any vapor there. We shall see more about this later.

We shall treat liquid and vapor as different species and specify the transition of

phases by a reaction rate equation. We introduce the following notation.

Quantities a_i denote the quantity for vapor when $i = 1$ and that of liquid when $i = 2$;

$f_i(x,t)$ is the volume fraction of ith species at point x and time t;

$\rho_i(x,t)$ is the density of ith species at point x and time t;

w_i is the reaction rate function denoting the mass of ith species produced per unit volume per time unit. By the conservation of mass, we have $w_1 + w_2 = 0$.

Modifying the systems of equations describing reacting two-phase flows, we derive the following balance laws to model the dynamics of phase transitions:

$$\begin{aligned}
&\rho_t + \nabla\cdot(\rho\mathbf{u}) = 0,\\
&(\rho_1 f_1)_t + \nabla\cdot(\rho_1 f_1\mathbf{u}) = w_1 + \nabla\cdot\left[\mu_{ii}\nabla\left(\frac{\rho_i f_i}{\rho}\right)\right],\\
&(\rho\mathbf{u})_t + \nabla\cdot(\rho(\mathbf{uu}) + \mathbf{P}) = 0,\\
&E_t + \nabla\cdot(\mathbf{u}E + \mathbf{u}\cdot\mathbf{P} + \mathbf{q}) = 0,
\end{aligned} \tag{2.1}$$

where $\mathbf{u}$ is the average velocity, E the energy per volume, $\mathbf{P}$ the stress tensor, $\mathbf{q}$ the heat flux vector, and μ the diffusion coefficients.

We make the following assumptions which simplify the modeling.

(A1) Vapor and liquid fill up the space, i.e.,

$$f_1 + f_2 = 1, \tag{2.2}$$

$$\rho = \rho_1 f_1 + \rho_2 f_2. \tag{2.3}$$

(A2) The temperatures of liquid and vapor components at each point are equal.

(A3) The pressure in the portion occupied by ith component is $p_i(\rho_i, T)$. Different components at the same location have the same pressure:

$$p = p_1(\rho_1, T) = p_2(\rho_2, T). \tag{2.4}$$

(A4) The stress tensor is

$$\mathbf{P} = \left[p + \left(\frac{2}{3}\epsilon_1 - \epsilon_2\right)(\nabla\cdot\mathbf{u})\right]\mathbf{I} - \epsilon_1(\nabla\mathbf{u} + \nabla\mathbf{u}^T) \tag{2.5}$$

and the heat conduction q is given by the Fourier law $q = -\kappa\nabla T$, where constants $\epsilon_1, \epsilon_2 > 0$, $\kappa > 0$ are viscosity and heat conductivity coefficients, respectively.

Under these assumptions, the system describing the dynamics of phase changes is

$$\begin{aligned}
&\rho_t + \nabla\cdot(\rho\mathbf{u}) = 0,\\
&(\rho_1 f_1)_t + \nabla\cdot(\rho_1 f_1\mathbf{u}) = w_1 + \nabla\cdot\left[\mu_{ii}\nabla\left(\frac{\rho_i f_i}{\rho}\right)\right],\\
&(\rho\mathbf{u})_t + \nabla\cdot(\rho(\mathbf{uu}) + \mathbf{P}) = 0,\\
&E_t + \nabla\cdot(\mathbf{u}E + \mathbf{u}\cdot\mathbf{P} + \mathbf{q}) = 0,\\
&p = p_1(\rho_1, T) = p_2(\rho_2, T),\\
&\rho = \rho_1 f_1 + \rho_2 f_2.
\end{aligned} \tag{2.6}$$

Once the relations $E = E(\rho, \rho_1 f_1, T)$ and $w_1 = w_1(\rho, \rho_1 f_1, T)$ are known, the system (2.6) forms a closed system of equations. In the one-dimensional case, this system is

reduced to

$$
\begin{aligned}
&\rho_t + (\rho u)_x = 0,\\
&(\rho u)_t + (\rho u^2 + p)_x = \epsilon u_{xx},\\
&E_t + (\rho u E + up - \epsilon u u_x - \kappa T_x)_x = 0,\\
&(\rho_1 f_1)_t + (\rho_1 f_1 u)_x = w_1 + \mu \left(\frac{\rho_1 f_1}{\rho}\right)_{xx},\\
&p = p_1(\rho_1, T) = p_2(\rho_2, T),\\
&\rho = \rho_1 f_1 + \rho_2 f_2.
\end{aligned} \tag{2.7}
$$

In Lagrange coordinates, the corresponding system of equations is

$$
\begin{aligned}
&v_t - u_x = 0,\\
&u_t + p_x = \epsilon \left(\frac{u_x}{v}\right)_x,\\
&e_t + (up)_x = \epsilon \left(\frac{u u_x}{v}\right)_x + \kappa \left(\frac{T_x}{v}\right)_x,\\
&\lambda_t = w(\lambda, v, T) + \mu \left(\frac{\lambda_x}{v}\right)_x,\\
&p = p_1(v_1, T) = p_2(v_2, T),\\
&v = \lambda v_1 + (1-\lambda) v_2,
\end{aligned} \tag{2.8}
$$

where $\lambda = \rho_1 f_1/\rho$ is the mass fraction of vapor in liquid/vapor mixture and $e = e(\lambda, v, T)$ is the specific energy and $w = w_1/\rho$. For the isothermal case, i.e., when the temperature is constant, which approximates the case where heat capacity is very large, the above system becomes

$$
\begin{aligned}
&v_t - u_x = 0,\\
&u_t + p_x = \epsilon \left(\frac{u_x}{v}\right)_x,\\
&\lambda_t = w(\lambda, v) + \mu \left(\frac{\lambda_x}{v}\right)_x,\\
&p = p_1(v_1) = p_2(v_2),\\
&v = \lambda v_1 + (1-\lambda) v_2.
\end{aligned} \tag{2.9}
$$

From the last two equations in (2.9), we find that if $\frac{\partial p_1}{\partial v}$, $\frac{\partial p_2}{\partial v} < 0$, then

$$
\frac{\partial p}{\partial v} = \frac{p_1'(v_1) p_2'(v_2)}{\lambda p_2'(v_2) + (1-\lambda) p_1'(v_1)} < 0 \tag{2.10}
$$

and

$$
\frac{\partial p}{\partial \lambda} = \frac{p_1'(v_1) p_2'(v_2)(v_2 - v_1)}{\lambda p_2'(v_2) + (1-\lambda) p_1'(v_1)} > 0. \tag{2.11}
$$

Further calculation shows that

$$
\frac{\partial^2 p}{\partial v^2} > 0 \text{ if } \frac{\partial^2 p_j}{\partial v^2} > 0, \qquad j = 1, 2. \tag{2.12}
$$

The production of vapor (or liquid) phase is through the initiation or annihilation of nuclei of vapor (or liquid) and the subsequent growth of such nuclei when these nuclei and elements of the metastable old phase meet. Correspondingly, the production rate function of the first species, w, contains two parts: the rate of the creation of nuclei of vapor phase, $w_{initiation}$, and that of the growth of such nuclei, w_{growth}. Similar to the theory of chemical kinetics and thermochemistry [see ZBLM], the part governing the growth of nuclei of vapor phase can be modeled by

$$w_{growth} = k\lambda^a(1-\lambda)^b,$$

where a and b are positive constants. In this paper, we shall take

$$w_{growth} = k\lambda(1-\lambda).$$

Here $\lambda(1-\lambda)$ is the probability for particles of liquid and vapor to collide to make reactions possible and k is known as the rate constant. In the theory of thermochemistry, the rate constant is a function of temperature given by Arrhenius's law. During liquid/vapor phase transitions, however, the temperature changes are usually minor, but the rate of phase change varies significantly according to $|p - p_e|$. Thus, the expression of the rate constant k should be adjusted according to the following facts: When $p_e(T) - p(\lambda, v, T) > 0$, where $p_e(T)$ is the equilibrium pressure at temperature T, liquid tends to evaporate and hence $w_{growth} \geq 0$ and the larger $p_e - p$, the faster the evaporation. Similarly, when $p_e(T) - p(\lambda, v, T) < 0$, vapor tends to condense into liquid and hence $w_{growth} \leq 0$ and the larger $|p_e - p|$, the faster the condensation. Consistent with these facts, we shall model the growth of nuclei of vapor by

$$w_{growth} = \frac{p_e - p}{\gamma p_e}\lambda(\lambda - 1), \tag{2.13}$$

where γ is taken as a constant.

The function $w_{initiation}$ is neglected in our study of traveling waves and Riemann problems. Thus, we do not discuss it here. For more information on this function, see the reviews [Ox, Sp] and references cited therein.

Remark. Now we return to our earlier discussion on the arbitrariness of the extension of the pressure functions beyond the spinodal point. We claim that the extension part of the pressure functions does not have much effect in our system. For example, let's consider the part of $p_1(\rho_1)$ in $\rho_1 > \alpha$. In this range, the rate function $w << -1$ has very large absolute value which forces the fraction of vapor λ to be virtually zero which implies that $\rho_2 = \rho > \beta$ and hence the pressure $p = p_2(\rho)$ is well defined and is not sensitive to the extended part of function p_1 for $\rho_1 > \alpha$. Thus the claim holds.

Remark. The diffusion term λ_{xx} has a significant role in system (2.9) and hence (2.6). The term $(p - p_e)\lambda(\lambda - 1)/\gamma/p_e$ represents the rate of reaction for liquid and vapor particles at the same location (x, t) only. It does not cover the reaction among neighboring particles. The diffusion term $\mu\lambda_{xx}$ then determines the chance for neighboring particles to collide. The necessity of this diffusion term can be illustrated by the following example. Let $u = 0$, $T =$ constant,

$$\lambda = \begin{cases} 0, & x < 0, \\ 1, & x \geq 0, \end{cases}$$

and v be such that pressure is a constant and the vapor is supersaturated at initial time. By Maxwell's rule, which states that the only stationary phase boundary happens at the equilibrium pressure, vapor should start to condense at the liquid/vapor

interface which results in the motion of the phase boundary. However, the system (2.9) with $\mu = 0$ says that the solution is the initial data and hence no phase change happens. In fact, we can see easily that when $\mu \neq 0$ and the pressure is not the equilibrium pressure, the liquid/vapor interface in (2.9) with $\mu > 0$ must move, which is in agreement with Maxwell's rule. In most traditional modeling of phase transitions in shock tube, droplet growth formulae are used which already include the effect of vapor near a droplet of liquid colliding with the droplet, resulting in the growth of the droplet. With the use of those droplet growth formulae, the diffusion term λ_{xx} is redundant. However, those droplet growth laws are usually difficult to analyze. Since we choose the simple form (2.13) for the rate function, the diffusion term is needed.

3. The existence of traveling waves. In this section, we shall provide sufficient conditions for the existence of traveling waves for (1.4) with (1.5), (1.6), and (1.7).

We modify the system of equations for traveling waves (1.9) as

$$\begin{aligned} &-cv' = c^2(v - v_-) + p - p_- + \eta v'', \\ &-c\lambda' = aw(v, \lambda) + b\lambda'', \\ &(v, \lambda)(-\infty) = (v_-, \lambda_-), \quad (v, \lambda)(\infty) = (v_+, \lambda_+). \end{aligned} \tag{3.1}$$

We intend to let the small constant $\eta > 0$ go to 0 after we establish the existence of solutions of (3.1). We see that there is a one-to-one correspondence between solutions of (3.1) with speeds $c > 0$ and those with negative speeds through the transformation $\xi \mapsto -\xi$. For this reason, we shall assume $c \geq 0$ in this section.

The system (3.1) ais the same system of equations of traveling waves with speeds c of the system

$$\begin{aligned} v_t &= \eta v_{xx} + c^2(v - v_-) + p - p_-, \\ \lambda_t &= b\lambda_{xx} + a(p - p_e)\lambda(\lambda - 1), \end{aligned} \tag{3.2}$$

or

$$U_t = AU_{xx} + F(U, c) \tag{3.2$'$}$$

for short, where $U = (v, \lambda)^T$, $A = \operatorname{diag}(\eta, b)$, and

$$F(U, c) = \begin{pmatrix} c^2(v - v_-) + p - p_- \\ a(p - p_e)\lambda(\lambda - 1) \end{pmatrix}. \tag{3.3}$$

The Jacobian of F is

$$\nabla F = \begin{pmatrix} c^2 + p_v & p_\lambda \\ ap_v\lambda(\lambda - 1) & a(p - p_e)(2\lambda - 1) + ap_\lambda\lambda(\lambda - 1) \end{pmatrix}. \tag{3.4}$$

The off-diagonal elements of ∇F are positive for $\lambda \in [0, 1]$. We recall that a system of reaction-diffusion equations

$$U_t = AU_{xx} + G(U) \tag{3.5}$$

is called monotone if all off-diagonal elements of ∇G are positive. Thus, the system (3.2) is a monotone system of parabolic partial differential equations for $\lambda \in [0, 1]$.

Now we consider the eigenvalues of ∇F at $(v_\pm, \lambda_\pm)$. By the Rankine–Hugoniot condition (1.10), we have $\lambda_\pm = 0, 1$ or $p(v_\pm, \lambda_\pm) = p_e$. When $\lambda_\pm = 0$ or 1, the eigenvalues of ∇F are

$$\alpha_{1\pm} = c^2 + p_v(v_\pm, \lambda_\pm) \tag{3.6a}$$

and

$$\alpha_{2\pm} = a(p_\pm - p_e)(2\lambda_\pm - 1). \tag{3.6b}$$

At $p = p_e$, the eigenvalues of ∇F are

$$\alpha_1 = \frac{1}{2}\left[c^2 + p_v + ap_\lambda\lambda(\lambda-1) + \sqrt{(c^2 + p_v + ap_\lambda\lambda(\lambda-1))^2 - 4ac^2p_\lambda\lambda(\lambda-1)}\right] \geq 0 \tag{3.6c}$$

and

$$\alpha_2 = \frac{1}{2}\left[c^2 + p_v + ap_\lambda\lambda(\lambda-1) - \sqrt{(c^2 + p_v + ap_\lambda\lambda(\lambda-1))^2 - 4ac^2p_\lambda\lambda(\lambda-1)}\right] \leq 0. \tag{3.6d}$$

According to the theory of traveling waves of monotone system (3.5), when some of the eigenvalues of ∇F at U_- are positive, there is no traveling wave of (3.3) with speed $c \geq 0$. The eigenvalues of ∇F at $U = U_-$ are negative if and only if either

$$\begin{aligned} &\alpha_{1-} = c^2 + p_{v-} < 0, \\ &p_- > p_e, \quad \lambda_- = 0, \end{aligned} \tag{3.7}$$

or

$$\begin{aligned} &\alpha_{1-} = c^2 + p_{v-} < 0, \\ &p_- < p_e, \quad \lambda_- = 1. \end{aligned} \tag{3.8}$$

We are interested in the existence of traveling waves when there are no equilibrium points (v^*, λ^*) of (1.9) with v^* between v_- and v_+. Then, by the Rankine–Hugoniot condition (1.10), possibilities for U_+ are as follows.

Case 1. Condition (3.7) and one of the following (1a) or (1b) hold:
(1a) $p_+ > p_e$, $\lambda_+ = 1$, $v_+ > v_-$, and $c^2 + p_{v+} < 0$.
(1b) $p_+ = p_e$, $\lambda_+ \in [0, 1]$, $v_+ > v_-$, and $c^2 + p_{v+} < 0$.
Case 2. Condition (3.8) and one of the following (2a) or (2b) hold:
(2a) $p_+ < p_e$, $\lambda_+ = 0$, $v_+ < v_-$, and $c^2 + p_{v+} < 0$.
(2b) $p_+ = p_e$, $\lambda_+ \in [0, 1]$, $v_+ < v_-$, and $c^2 + p_{v+} < 0$.
Case 3. Condition (3.7) and one of the following (3a) or (3b) hold:
(3a) $p_+ < p_-$, $\lambda_+ = 0$, and $v_+ > v_-$.
(3b) $p_+ > p_-$, $\lambda_+ = 0$, and $v_+ < v_-$.
Case 4. Condition (3.8) and one of the following (4a) or (4b) hold:
(4a) $p_+ < p_-$, $\lambda_+ = 1$, and $v_+ > v_-$.
(4b) $p_+ > p_-$, $\lambda_+ = 1$, and $v_+ < v_-$.

Cases (3b) and (4b) are not possible for traveling waves of nonnegative speed. Cases (3a) and (4a) correspond to ordinary Lax shock without phase transitions. Our interest is in Case 1 and Case 2, which involve phase changes. We list cases corresponding to Case 1 and Case 2 for negative speed.

Case 1′. The conditions

$$c^2 + p_{v+} < 0, \quad p_+ > p_e, \quad \lambda_+ = 0 \tag{3.7′}$$

and either (1′a) $p_- > p_e$, $\lambda_- = 1$, and $v_- > v_+$, or (1′b) $p_- = p_e$, $\lambda_- \in [0,1]$, and $v_+ < v_-$ hold.

Case 2′. The conditions

$$c^2 + p_{v+} < 0, \quad p_+ < p_e, \quad \lambda_+ = 1 \tag{3.8′}$$

and either (2′a) $p_- < p_e$, $\lambda_- = 0$ and $v_+ > v_-$, or (2′b) $p_- = p_e$, $\lambda_- \in [0,1]$, and $v_+ > v_-$ hold.

In Cases 1 and 2, eigenvalues of ∇F at U_- are negative. At U_+, one eigenvalue of ∇F is nonpositive and the other is positive. In other words, U_- is a stable equilibrium of (3.3) while U_+ is an unstable equilibrium. Thus, system (3.3) in Cases 1 and 2 is monostable.

We are interested in monotone traveling waves of (3.4). We say that a vector-valued function is monotone if every component of the vector-valued function is monotone. When we say a vector $q \geq 0$, we mean that each of its components is nonnegative. An interval $[U, W]$, where U and W are two vectors of the same size, is the set of all vectors q satisfying $U \leq q \leq W$.

THEOREM 3.1. (see [VVV, Chapter 3, Theorem 4.3]). *Let the system* (3.5) *be monotone and monostable with U_+ being the unstable equilibrium. Assume that a vector $q \geq 0$ exists such that*

$$G(rq + U_+) \geq 0 \quad \text{for } 0 \leq r \leq r_0, \tag{3.9}$$

where $r_0 > 0$ is some number. Assume that in the interval $[U_+, U_-]$, the vector-valued function $G(U)$ vanishes only at U_+ and U_-. Suppose the matrix A in (3.5) *is $A = \operatorname{diag}(a_1, a_2)$ with $a_1, a_2 > 0$. Then for all*

$$s \geq \omega := \inf_{U \in K} \sup_{x,j} \frac{a_j U_j'' + G_j(U)}{-U_j'} \tag{3.10}$$

there exists a decreasing traveling wave of (3.5) *with speed $s \geq 0$, where*

$$K := \left\{ U \in C^2(\mathbb{R}; \mathbb{R}^2) \mid U \text{ is decreasing and } \lim_{x \to \pm\infty} U(x) = U_\pm \right\}.$$

When $s < \omega$ such a solution does not exist.

By performing the transformation

$$\bar{U} = -U,$$
$$\bar{G}(\bar{U}) = -G(-\bar{U}).$$

Theorem 3.1 can be rewritten as follows to allow $U_+ > U_-$.

THEOREM 3.1′. *Let the system* (3.5) *be monotone and monostable with U_+ being the unstable equilibrium. Assume that a vector $q \leq 0$ exists such that*

$$G(rq + U_+) \leq 0 \quad \text{for } 0 \leq r \leq r_0, \tag{3.9′}$$

where $r_0 > 0$ is some number. Assume that $G(U) \neq 0$ in the interval $[U_-, U_+]$. Suppose the matrix A in (3.5) *is $A = \operatorname{diag}(a_1, a_2)$ with $a_1, a_2 > 0$. Then system* (3.5) *has an increasing traveling wave with speed $s \geq 0$ if and only if*

$$s \geq \omega := \inf_{U \in K'} \sup_{x,j} \frac{a_j U_j'' + G_j(U)}{-U_j'}, \tag{3.10′}$$

where

$$K' := \{U \in C^2(\mathbb{R};\mathbb{R}^2) \mid U \text{ is increasing and } \lim_{x\to\pm\infty} U(x) = U_\pm\}.$$

We have to bear in mind that we are looking for traveling waves of (3.3) with speed $c > 0$ and where $F(U, c)$, unlike $G(U)$ in (3.5), contains c. Thus, to prove (3.1) has a solution, it is necessary and sufficient to prove that $c \geq \omega(c)$, where $\omega(c)$ is defined as in (3.10) with $G(U)$ replaced by $F(U, c)$.

THEOREM 3.2. *For Cases* 1 *and* 2, *if*

$$c \geq \omega^* := 2\sqrt{ab|p_- - p_e|}, \tag{3.11}$$

then there is a solution of (3.1) *for* $\eta > 0$ *small enough. For Case* $1'$ *and* $2'$, *if*

$$-c \geq \omega^* := 2\sqrt{ab|p_+ - p_e|}, \tag{3.11$'$}$$

then there is a solution of (3.1) *for* $\eta > 0$ *small enough.*

Proof. We consider Case 2, that is,

$$c^2 + p_{v\pm} < 0, \quad U_+ = (v_+, \lambda_+) < (v_-, \lambda_-) = (v_-, 1) = U_-, \quad p_- < p_+ \leq p_e, \tag{3.12}$$

where $\lambda_+ \in [0, 1)$ and there is no other equilibrium point with v between $v_\pm$. The proof for Case 1 is similar.

By assumptions (1.5) and (3.12), we see that there is no equilibrium point in the interval (U_+, U_-). Now we verify the condition (3.9). In fact, we can take the vector $q = (q_1, q_2)^T > (0, 0)^T$ so that

$$0 < -\frac{(c^2 + p_{v+})q_1}{p_{\lambda+}} < q_2 < -\frac{p_{v+}q_1}{p_{\lambda+}}. \tag{3.13}$$

With (3.13), we have

$$\left[\frac{d}{dr}p(rq_1 + v_+, rq_2 + \lambda_+)\right]\Bigg|_{r=0} = p_{v+}q_1 + p_{\lambda+}q_2 < 0, \tag{3.14}$$

which implies that $p(rq+U_+) < p_+ < p_e$ for small $r > 0$. Thus, the second component of F in (3.3)

$$F_2(rq + U_+, c) = a(p(rq + U_+) - p_e)(rq_2 + \lambda_+)(rq_2 + \lambda_+ - 1) > 0 \tag{3.15}$$

for small $r > 0$. Similarly, by using Rankine–Hugoniot condition (1.11), we can write the first component of F as

$$F_1(rq + U_+, c) = c^2 rq_1 + p(rq + U_+) - p_+.$$

Its derivative satisfies

$$\frac{dF_1}{dr}\Bigg|_{r=0} = (c^2 + p_{v+})q_1 + p_{\lambda+}q_2 > 0$$

under the choice (3.13). This implies that $F_1(rq + U_+, c) > 0$ for small $r > 0$. Thus, condition (3.9) is satisfied by $F(U, c)$ in Case 2.

From Theorem 3.1, we know that (3.2) has a decreasing traveling wave with speed $c > 0$ if and only if

$$c \geq \omega(c) = \inf_{U\in K} \sup_{x,j} \frac{a_j\rho'' + F_j(\rho, c)}{-\rho_j'}.$$

Since $j = 1, 2$ in the above, we can consider $j = 1$ and 2 separately. We start with $j = 2$ since in this case

$$\omega_2(c) := \inf_{(v,\lambda)\in K} \sup_x \frac{b\lambda'' + a(p - p_e)\lambda(\lambda - 1)}{-\lambda'} \tag{3.16}$$

does not contain c explicitly. By Lemma 3.3 below, given a function

$$\lambda(x) \in K_2 := \{\lambda \in C^2(\mathbb{R};\mathbb{R}) \mid \lambda(x) \text{ is decreasing and } \lim_{x\to\pm\infty} \lambda(x) = \lambda_\pm\}, \tag{3.17}$$

we can select a function $v(x) = v(\lambda(x))$ so that

$$p(v(x), \lambda(x)) \in [p_-, p_+]. \tag{3.18}$$

We note that K_2 is the set of functions which are the second component of functions in K. For such a function $U(x) = (v(\lambda(x)), \lambda(x))$, we have

$$\omega_2(c) \le \inf_{\lambda\in K_2} \sup_x \frac{b\lambda'' + a(p_- - p_e)\lambda(\lambda - 1)}{-\lambda'} =: \omega^*. \tag{3.19a}$$

It is clear that ω^* is independent of c. Now we consider

$$\omega_1(c) := \inf_{(v,\lambda)\in K} \sup_x \frac{\eta v'' + c^2(v - v_+) + p - p_+}{-v'}. \tag{3.19b}$$

Suppose that $\lambda_n(x)$, $n = 1, 2, 3, \ldots$ is a sequence of functions in K_2 satisfying

$$\omega^* + 1 > \sup_x \frac{b\lambda_n'' + a(p_- - p_e)\lambda_n(\lambda_n - 1)}{-\lambda_n'} \to \omega^* \tag{3.20}$$

as $n \to \infty$. Now we need the following lemma whose proof will follow this one.

LEMMA 3.3. *Let $(v_\pm, \lambda_\pm)$ be of Case 2. For each of the functions $\lambda_n(x)$, $n = 1, 2, 3, \ldots$, in K_2 satisfying* (3.20)*, the equation*

$$R := c^2(v - v_+) + p(v, \lambda_n) - p_+ = 0 \tag{3.21}$$

uniquely defines a function $v_n(x)$ such that $(v_n, \lambda_n) \in K$. Furthermore, the functions $(v_n(x), \lambda_n(x))$ satisfy $p(v_n(x), \lambda_n(x)) \in [p_-, p_+]$ and

$$0 \le \sup_x \frac{v_n''}{-v_n'} \le C \tag{3.22}$$

for some constant $C > 0$ independent of n.

With these functions (v_n, λ_n), we see that

$$\omega_1(c) \le \inf_n \sup_x \frac{\eta v_n''}{-v_n'} = O(1)\eta. \tag{3.23}$$

It is clear that

$$\omega(c) = \max(\omega_1(c), \omega_2(c))$$

holds. With $\eta > 0$ small enough, we have from above (3.19a) and (3.23) that

$$\omega(c) = \omega_2 \le \omega^*. \tag{3.24}$$

Therefore, if $c \geq \omega^*$, there is a solution of (3.1) for sufficiently small $\eta > 0$.

To complete the proof of the first statement of the theorem, it remains to prove that $\omega^* = 2\sqrt{ab|p_- - p_e|}$. To this end, we consider the equation

$$\lambda_t = b\lambda_{xx} + a(p_- - p_e)\lambda(\lambda - 1) \tag{3.25}$$

and its traveling wave equations

$$\begin{aligned} &-c\lambda' = b\lambda'' + a(p_- - p_e)\lambda(\lambda - 1), \\ &\lambda(-\infty) = 1, \quad \lambda(\infty) = 0. \end{aligned} \tag{3.26}$$

It can be verified that (3.25) satisfies the conditions of Theorem 3.1. Then, (3.26) has a monotone solution if and only if $c \geq \omega^*$. We claim that (3.26) has a solution if and only if $c \geq 2\sqrt{ab|p_- - p_e|}$. It is clear that this claim implies $\omega^* = 2\sqrt{ab|p_- - p_e|}$ in view of Theorem 3.1. To prove this claim, we observe that (3.26) is equivalent to

$$\begin{aligned} &\lambda' = q, \\ &bq' = -cq - a(p_- - p_e)\lambda(\lambda - 1), \\ &(\lambda, q)(-\infty) = (1, 0), \quad (\lambda, q)(\infty) = (0, 0). \end{aligned} \tag{3.27}$$

The eigenvalues of (3.27) at $(\lambda, q) = (1, 0)$ are

$$\alpha_{1-} = \frac{1}{2b}[-c - \sqrt{c^2 - 4ab(p_- - p_e)}] < 0$$

and

$$\alpha_{2-} = \frac{1}{2b}[-c + \sqrt{c^2 - 4ab(p_- - p_e)}] > 0,$$

where we used $p_- - p_e < 0$ in Case 2. There is an unstable manifold of (3.27) issued from $(\lambda = 1, q = 0)$ into the triangle in (λ, q)-plane:

$$D := \left\{ (\lambda, q) \in \mathbb{R}^2 \ : \ 0 \leq \lambda \leq 1, \ -\frac{c}{2b}\lambda \leq q \leq 0 \right\}. \tag{3.28}$$

By (3.27), this unstable manifold cannot cross the boundary of D at $q = 0$, $0 \leq \lambda \leq 1$. At the part of the boundary of D, $q = -\frac{c}{2b}\lambda$, the slope of the unstable manifold can be calculated from (3.27):

$$\begin{aligned} \frac{dq}{d\lambda} &= -\frac{c}{b} - \frac{a(p_- - p_e)\lambda(\lambda - 1)}{bq} \\ &= -\frac{c}{2b} + \frac{2a(p_- - p_e)(\lambda - 1)}{c} - \frac{c}{2b} \\ &= -\frac{1}{2bc}(c^2 - 4ab(p_- - p_e)(\lambda - 1)) - \frac{c}{2b} \\ &\leq -\frac{1}{2bc}(c^2 - 4ab|p_- - p_e|) - \frac{c}{2b}, \end{aligned} \tag{3.29}$$

where we used $p_- - p_e < 0$ in the last step. If

$$c \geq 2\sqrt{ab|p_- - p_e|},$$

then

$$\frac{dq}{d\lambda} \le -\frac{c}{2b},$$

which implies that the unstable manifold cannot cross the boundary of D. Thus, this unstable manifold has to enter $(\lambda, q) = (0, 0)$ as $\xi \to \infty$ and hence there is a solution of (3.26) when $c \ge 2\sqrt{ab|p_- - p_e|}$. On the other hand, the eigenvalues of (3.27) at $\lambda = 0$ are

$$\alpha = \frac{1}{2b}\Big[-c \pm \sqrt{c^2 - 4ab|p_- - p_e|}\Big],$$

which are imaginary if $c < 2\sqrt{ab|p_- - p_e|}$. Then the stable manifold of (3.27) at $(0, 0)$ is not monotone and hence there is no monotone solution of (3.26). In view of Theorem 3.1, $\omega^* = 2\sqrt{ab|p_- - p_e|}$. This completes the proof of the first statement.

The proof for Case 1 is similar. The only difference is that we use Theorem 3.1′ instead of Theorem 3.1. Performing a transform $\xi \mapsto -\xi$, we can convert our statements for Cases 1 and 2 to those for Cases 1′ and 2′. □

Proof of Lemma 3.3. First, we prove that for each $\lambda \in [\lambda_+, \lambda_- = 1]$, the solution v of (3.21)

$$R(v, \lambda) := c^2(v - v_+) + p(v, \lambda) - p_+ = 0 \tag{3.30}$$

in the range $[v_+, v_-]$ is unique. Indeed, if otherwise, there would be a number $\lambda_0 \in [\lambda_+, \lambda_-]$ such that $R(v, \lambda_0) = 0$ has two solutions v_0 and v_1, with $v_0 < v_1$. Since

$$R_{vv} = p_{vv} > 0, \tag{3.31}$$

it is necessary that

$$R_v(v_0, \lambda_0) < 0 \text{ and } R_v(v_1, \lambda_0) > 0 \tag{3.32}$$

and that

$$R_v(v, \lambda_0) > R_v(v_1, \lambda_0) > 0 \quad \text{for } v_- > v > v_1. \tag{3.33}$$

Inequality (3.33) then implies that $0 = R(v_-, \lambda_-) > R(v_-, \lambda_0) > R(v_1, \lambda_0) = 0$ which is a contradiction. This contradiction establishes the uniqueness of the solution of (3.30) in the range $v \in [v_+, v_-]$.

The above argument also implies that if $R(v, \lambda) = 0$ with $\lambda \in [\lambda_+, \lambda_-]$ and $v \in [v_+, v_-]$, then at such (v, λ),

$$R_v = c^2 + p_v < 0. \tag{3.34}$$

For $\lambda(x) \in [\lambda_+, \lambda_-]$, we have that

$$R(v_+, \lambda(x)) > R(v_+, \lambda_+) = 0 = R(v_-, \lambda_-) > R(v_-, \lambda(x)). \tag{3.35}$$

Thus, there is a unique function $v(x)$ satisfying $R(v(x), \lambda(x))$. If $\lambda(x)$ is in K_2, that is, $\lambda \in C^2(\mathbb{R}; \mathbb{R})$, $\lambda' < 0$, $\lambda(x) \to \lambda_\pm$ as $x \to \pm\infty$, then

$$v' = -\frac{p_\lambda \lambda'}{c^2 + p_v} < 0, \tag{3.36}$$

where we used (3.34). Further computation shows that $v \in C^2(\mathbb{R};\mathbb{R})$ and $v(x) \to v_\pm$ as $x \to \pm\infty$. In other words, $(v,\lambda)(x)$ determined by $R = 0$ is in K if $\lambda(x)$ is in K_2.

Observing that the solution of equation $R = 0$ is the intersection of a straight line $p = -c^2(v - v_+) + p_+$ and the curve $p = p(v,\lambda)$ in (v,p)-plane, we see that the solution of $R(v,\lambda(x)) = 0$ satisfies (3.18),

$$p(v(x),\lambda(x)) \in [p_-, p_+]. \tag{3.37}$$

Now we consider $-v_n''/v_n'$ for function v_n satisfying (3.20). We claim $||\lambda_n'||_\infty$ is independent of n. Indeed, if otherwise, there is a subsequence of $\{\lambda_n\}$, still denoted by $\{\lambda_n\}$ such that $||\lambda_n'||_\infty \to \infty$ as $n \to \infty$. By the fact that $\lambda(x) \in [\lambda_+, \lambda_-]$, there is an interval $[y_n, x_n]$ such that

$$\lim_{n\to\infty} \lambda_n'(y_n) = -\infty \tag{3.38}$$

and

$$-\lambda_n'(x) \geq -\lambda_n'(x_n) = 1 \quad \text{for } x \in [y_n, x_n]. \tag{3.39}$$

By the monotonicity of $\lambda(x)$, it is clear that

$$|y_n - x_n| \leq 1/|\lambda_- - \lambda_+|. \tag{3.40}$$

On the interval $[y_n, x_n]$, from (3.20), (3.37), and (3.39), we have

$$\frac{\lambda_n''}{-\lambda_n'} = C_n(x) \leq C, \tag{3.41}$$

where $C > 0$ is a constant independent of n. Integrating (3.41), we obtain

$$|\lambda_n'(y_n)| = |\lambda_n'(x_n)| \exp\left(\int_{y_n}^{x_n} C(x)dx\right) \leq C$$

which contradicts (3.38). Thus, we have

$$||\lambda_n'||_\infty \leq C. \tag{3.42}$$

From (3.30), we have

$$v_n' = -\frac{p_\lambda}{c^2 + p_v}\lambda_n'. \tag{3.43}$$

From (3.34), we know that $c^2 + p_v < 0$ for (v,λ) satisfying (3.30) in the range $\lambda \in [\lambda_+, \lambda_-]$ and $v \in [v_+, v_-]$. Then there is a constant δ_0 such that

$$c^2 + p_v < -\delta_0. \tag{3.44}$$

Applying this and (3.42) in (3.43), we obtain

$$||v_n'||_\infty \leq C. \tag{3.45}$$

To prove (3.22), we compute from (3.30) to get

$$\begin{aligned}\frac{v_n''}{-v_n'} &= \frac{1}{c^2+p_v}\left[p_{vv}v_n' + 2p_{v\lambda}\lambda_n' + \frac{p_{\lambda\lambda}(c^2+p_v)}{p_\lambda}\lambda_n' + p_\lambda\frac{\lambda_n''}{\lambda_n'}\right]\\ &\le C + \frac{p_\lambda}{c^2+p_v}\frac{\lambda_n''}{\lambda_n'}\\ &\le C - \frac{p_\lambda}{b(c^2+p_v)}\left[\frac{b\lambda_n'' + a(p_- - p_e)\lambda(\lambda-1)}{-\lambda_n'} - \frac{a(p_- - p_e)\lambda(\lambda-1)}{-\lambda_n'}\right]\\ &\le C - \frac{p_\lambda}{b(c^2+p_v)}\left[\frac{b\lambda_n'' + a(p_- - p_e)\lambda(\lambda-1)}{-\lambda_n'}\right] \le C,\end{aligned}$$

where we used (3.20) and the facts that $p_- < p_e$, $c^2 + p_v < -\delta_0$, and $\lambda_n' < 0$. The part (3.22), $0 \le \sup_x(-v\prime\prime_n/v_n')$, is a direct consequence of $v_n' < 0$ and $v_n(x) \to v_\pm$ as $x \to \pm\infty$. □

THEOREM 3.4. *Assume the data $(v_\pm, \lambda_\pm)$ are of one of Case* 1 *or Case* 2.

(i) *If the speed c of traveling waves satisfies*

$$c \ge \omega^* := 2\sqrt{ab|p_- - p_e|}, \tag{3.46}$$

then there is a traveling wave solution of (1.9). *If the speed c satisfies*

$$c < 2\sqrt{ab|p_+ - p_e|}, \tag{3.47}$$

then there is no traveling wave of (1.9) *satisfying* $\lambda \in [0,1]$.

(ii) *For Cases* $1'$ *and* $2'$, *if*

$$-c \ge \omega^* := 2\sqrt{ab|p_+ - p_e|}, \tag{3.46$'$}$$

then there is a traveling wave solution of (1.9). *If the speed c satisfies*

$$-c < 2\sqrt{ab|p_- - p_e|}, \tag{3.47$'$}$$

then there is no traveling wave of (1.9) *satisfying* $\lambda \in [0,1]$.

Proof. (i) From Theorem 3.2, we see that under condition (3.46), there is a monotone solution of (3.1) with sufficiently small $\eta > 0$. We denote this solution by (v^η, λ^η). We choose arbitrarily a fixed number λ_0 between $\lambda_\pm$ and not equal to $\lambda_\pm$. Since (3.1) is invariant under shifting, $\xi \mapsto \xi + \xi_0$, we can assume $\lambda^\eta(0) = \lambda_0$. By the monotonicity and boundedness of (v^η, λ^η), there is a sequence $\{\eta_n\}_{n=1}^\infty$ such that $\eta_n \to 0+$ as $n \to \infty$ and

$$(v,\lambda)(\xi) := \lim_{n\to\infty}(v^{\eta_n}, \lambda^{\eta_n})(\xi) \tag{3.48}$$

exists. The limit $(v,\lambda)(\xi)$ defined in (3.48) satisfies $(1.9)_1$ and $(1.9)_2$ weakly. A weak solution of $(1.9)_1$ and $(1.9)_2$ is also a strong solution. It is clear that the limit $(v,\lambda)(\xi)$ is monotone and is contained in the interval $[(v_+,\lambda_+),(v_-,\lambda_-)]$ and satisfies $\lambda(0) = \lambda_0$. Since the interior of the interval $[(v_+,\lambda_+),(v_-,\lambda_-)]$ does not contain equilibrium point of (1.9), the boundary condition $(1.9)_3$ is also satisfied by the limit $(v,\lambda)(\xi)$. Thus, $(v,\lambda)(\xi)$ is a solution of (1.9).

For definiteness, we consider Case 1 in our proof for the second statement in (i). In this case, condition (3.47) implies that $p_- > p_+ > p_e$ and hence $\lambda_+ = 1$. The eigenvalues of (1.9) at (v_+,λ_+) are

$$\alpha_{1+} = -\frac{c^2 + p_{v+}}{-c} > 0$$

and

$$\alpha_{2+} = \frac{1}{2b}\Big[-c \pm \sqrt{c^2 - 4ab|p_+ - p_e|}\Big].$$

Under condition (3.47), α_{2+} are complex. Thus, stable manifolds of (1.9) at (v_+, λ_+) have a part in the region $\lambda > 1$ and hence there is no solution of (1.9) satisfying $\lambda \in [0, 1]$. The proof for Case 2 is similar.

Statement (ii) can be proved similarly. □

Remark. It is clear from (3.24) that $\omega(c)$ is determined by the reaction-diffusion part of the system (1.4). In this sense, we can say that the existence of traveling waves of (1.4) is primarily determined by $(1.4)_3$.

COROLLARY 3.5. (i) *Let $\lambda_- = 0$ or 1. For each (v_-, λ_-), if $ab > 0$ are small enough, then there are (v_+, λ_+) such that $(v_\pm, \lambda_\pm)$ are of Case 1 or 2 for which there is a solution to the traveling wave equation* (1.9) *with speed $c > 0$.*

(ii) *Let $\lambda_+ = 0$ or 1. For each (v_+, λ_+), if $ab > 0$ are small enough, then there are (v_-, λ_-) such that $(v_\pm, \lambda_\pm)$ are of Case $1'$ or $2'$ for which there is a solution to the traveling wave equation* (1.9) *with $c < 0$.*

Proof. (i) For definiteness, we consider only Case 1, where $\lambda_- = 0$ and $p_- > p_+ \geq p_e$. The proof for Case 2 is similar. From Theorem 3.4, we know that if $1 \geq c^{-2} 4ab(p_- - p_e)$ or equivalently

$$1 \geq 4ab\frac{v_+ - v_-}{p_- - p_+}(p_- - p_e), \tag{3.49}$$

then there is a solution of (1.9). Since $p_+ > p_e$, we have $v_+ \leq M$, the Maxwell point at which $p(M, 1) = p_e$. We can choose v_+ so that p_+ is close to p_e. Then for small enough $ab > 0$, the left-hand side of (3.49) satisfies

$$4ab\frac{v_+ - v_-}{p_- - p_+}(p_- - p_e) \leq 4ab(M - v_-) \leq 1 \tag{3.50}$$

and hence there are solutions of (1.9) for such $(v_\pm, \lambda_\pm)$.

(ii) The proof is similar to that of (i). □

From Theorem 3.4 or Corollary 3.5, we see that for some (v_-, λ_-), there are infinitely many (v_+, λ_+) so that the traveling wave equation (1.9) has a solution. If all these traveling waves are "good," then solutions of a Riemann problem for (1.4) in the $\epsilon \to 0+$ limit will be nonunique. We say that a traveling wave of (1.4) is metastable if it is stable with respect to perturbations in (u, v) but not in λ. Only stable or metastable traveling waves can be present in a solution for a sizable period of time. Thus, only stable or metastable traveling waves of (1.4) are considered as admissible traveling waves. The stability and admissibility of traveling waves of (1.4) is left for future investigations.

4. Wave patterns in solutions to some Riemann problems and those observed in experiments on retrograde fluids. In this section, we shall investigate solutions to Riemann problems of (1.4) with (1.5), (1.6), and (1.7) in the $\epsilon \to 0+$ limit with scaling $\gamma = a\epsilon$ and $\mu = b\epsilon$. We show that system (1.4) can exhibit major one-dimensional wave patterns of liquid/vapor phase transitions observed in shock tube experiments for retrograde fluids, i.e., fluids with large heat capacity. We shall also discuss the order of magnitude of the possible error between computation and experimental data due to the modeling.

Major one-dimensional wave patterns observed in shock tube experiments on retrograde fluids are listed in (a)–(c) in section 1. We are interested in whether these wave patterns can be observed in solutions of the initial value problem

$$\begin{aligned} v_t - u_x &= 0, \\ u_t + p(v,\lambda)_x &= \epsilon u_{xx}, \\ \lambda_t &= \frac{a}{\epsilon}(p-p_e)\lambda(\lambda-1) + b\epsilon\lambda_{xx}, \\ (u,v,\lambda)(x,0) &= \begin{cases} (u_-,v_-,\lambda_-) & \text{if } x<0, \\ (u_+,v_+,\lambda_+) & \text{if } x>0, \end{cases} \end{aligned} \tag{4.1}$$

when $\epsilon > 0$ is small. We denote the solution of (4.1) by $(u^\epsilon, v^\epsilon, \lambda^\epsilon)(x,t)$. If there is a sequence ϵ_n, $n = 1, 2, \ldots$, such that $\epsilon_n \to 0+$ as $n \to \infty$ and the limit

$$(u,v,\lambda)(x,t) := \lim_{n\to\infty} (u^{\epsilon_n}, v^{\epsilon_n}, \lambda^{\epsilon_n})(x,t) \tag{4.2}$$

exists almost everywhere, then the limit satisfies

$$\begin{aligned} &v_t - u_x = 0, \\ &u_t + p(v,\lambda(x,t))_x = 0, \\ &(p(v,\lambda)-p_e)\lambda(\lambda-1) = 0, \\ &(u,v,\lambda)(x,0) = \begin{cases} (u_-,v_-,\lambda_-) & \text{if } x<0, \\ (u_+,v_+,\lambda_+) & \text{if } x>0. \end{cases} \end{aligned} \tag{4.3}$$

Instead of studying (4.1) for small $\epsilon > 0$ directly, we can study solutions of (4.3) that are $\epsilon \to 0+$ limits of solutions of (4.1). Thus, we are interested in solutions of (4.3) that are some type of strong limits of solutions of (4.1) as $\epsilon_n \to 0$ for some sequence $\{\epsilon_n\}$. Also, since only stable or metastable solutions can be observed, we allow only stable or metastable solutions as admissible. A solution is called metastable if it is stable with perturbations in u and v only.

DEFINITION 4.1. *If a stable or metastable solution $(u,v,\lambda)(x,t)$ of (4.3) is a strong limit of $(u^{\epsilon_n}, v^{\epsilon_n}, \lambda^{\epsilon_n})$, solutions of (4.1) with $\epsilon = \epsilon_n$, for some sequence $\{\epsilon_n\}_{n=1}^\infty$, $\epsilon_n \to 0+$ as $n \to \infty$, then we call $(u,v,\lambda)(x,t)$ an admissible solution of (4.3).*

From $(4.3)_3$, piecewise smooth solutions of (4.3) consist of (a) shock waves with two sides of the shock satisfying $\lambda = 0, 1$ or $p = p_e$, (b) smooth waves with $\lambda \equiv 0$ or 1, and (c) smooth isobaric waves where $p = p_e$.

(a) Shock waves. We say that a shock with end states $(u_\pm, v_\pm, \lambda_\pm)$ has a shock profile if the traveling wave equation (1.9) of (4.1) has a solution with $(v,\lambda)(\pm\infty) = (v_\pm, \lambda_\pm)$.

When $\lambda_+ \neq \lambda_-$, there is a phase change across the shock. Sufficient conditions for the existence of shock profiles for such shocks are given in Theorem 3.4 and Corollary 3.5. The stability or metastability of these profiles is left for future investigations.

For shocks with $\lambda_+ = \lambda_-$, there is no phase transition involved. From (4.1), we can see that it is necessary that $\lambda_- = \lambda_+ = 0$, or 1 in this case. The admissibility for these nonreacting shocks is determined by Lax's criterion. Nonreacting shock profiles satisfying Lax's criterion are metastable; see [SX].

(b) Nonreacting smooth rarefaction waves. These are the "ordinary" admissible gas dynamic rarefaction waves with $\lambda \equiv 0$ or $\lambda \equiv 1$. These nonreacting rarefaction waves are metastable; see [X].

(c) Isobaric waves. These are smooth solutions of (4.3) with

$$p(v(x,t),\lambda(x,t)) = p_e \tag{4.4}$$

for (x,t) in some regions D called isobaric regions. In isobaric regions, (4.3) and (4.4) yield

$$\begin{aligned} &u = u(x,t_0),\\ &v(x,t) = v_t(x,t_0)(t-t_0) + v(x,t_0),\\ &\lambda = \lambda_e(v(x,t)), \end{aligned} \tag{4.5}$$

where the last equation is the explicit form of (4.4), which exists due to $p_\lambda > 0$. The characterization of admissible isobaric solutions of (4.3) is left for future investigations.

From the above discussions, we can define admissible piecewise smooth solutions as follows.

DEFINITION 4.2. (i) *A shock wave solution of* (4.3) *is admissible if the shock has a stable or metastable traveling wave profile.*

(ii) *A piecewise smooth solution of* (4.3) *is admissible if all its discontinuities have stable or metastable shock profiles and all smooth parts of the solution are either nonreacting rarefaction waves or isobaric waves admissible in the sense of Definition* 4.1.

The following are examples of Riemann problems of (4.3) exhibiting wave patterns observed in shock tube experiments on retrograde fluids.

Example 4.1. This example shows that solutions of Riemann problems of (4.3) can exhibit the wave splitting phenomena as depicted by Figure 1.2(b). The compression shock is set by the initial condition

$$(u,v,\lambda)(x,0) = \begin{cases} (u_- > 0, v_-, \lambda_- = 0) & \text{if } x < 0,\\ (u_+ = 0, v_+, \lambda_+ = 1) & \text{if } x > 0 \end{cases} \tag{4.6}$$

with $v_- < v_+$ and $p(v_+,\lambda_+) < p_e < p(v_-,\lambda_-)$.

In these initial data, the fluid is stable vapor at rest for $x > 0$ and stable liquid for $x < 0$ moving from left to right.

We assume that $p_{vv} > 0$. From the classical theory of the Riemann problem of the p-system for isothermal gas dynamics, we know that the states $(u_*, v_*, \lambda_* = 0)$ that can connect $(u_-, v_-, \lambda_- = 0)$ from the right by backward nonreacting shocks are determined by

$$S_1: \qquad u_* - u_- = -\sqrt{(v_* - v_-)(p_- - p_*)}, \quad \alpha \geq v_- > v_*, \tag{4.7}$$

while those by backward rarefaction waves are given by

$$R_1: \qquad u_* - u_- = \int_{v_-}^{v_*} \sqrt{-p_v(y,0)}\,dy, \quad v_- < v_* \leq \alpha. \tag{4.8}$$

Those states $(u^*, v^*, \lambda^* = 1)$ that can connect $(u_+, v_+, \lambda_+ = 1)$ from the left by forward nonreacting shocks and rarefaction waves are determined by

$$S_2: \qquad u^* - u_+ = \sqrt{(v^* - v_+)(p_+ - p^*)}, \quad \beta \leq v^* < v_+ \tag{4.9}$$

and

$$R_2: \qquad u_+ - u^* = \int_{v^*}^{v_+} \sqrt{-p_v(y,0)}\,dy, \quad v^* > v_+ \geq \beta, \tag{4.10}$$

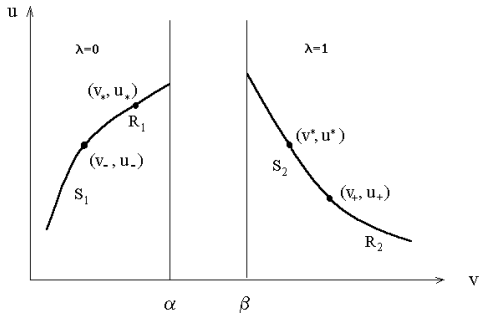

FIG. 4.1(a). *The curves S_1 and R_1 are the set of points that can be connected to (u_-, v_-) from the right by a backward shock and a backward rarefaction wave, respectively. The curves S_2 and R_2 are the set of points that can be connected to (u_+, v_+) from the left by a forward shock and a forward rarefaction wave, respectively.*

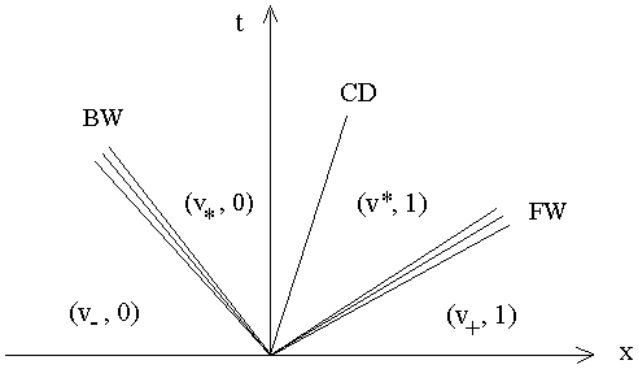

FIG. 4.1(b). *BW is a backward nonreacting shock or rarefaction wave. CD is a condensation discontinuity. FW is a forward nonreacting shock or rarefaction wave.*

respectively; see Figure 4.1(a). Then the structure of the general solution of the Riemann problem with initial data (4.6) is as shown in Figures 4.1(a) and 4.1(b) which consists of, from left to right, a backward nonreacting shock or rarefaction wave, BW, followed by a condensation discontinuity, CD, and a faster moving forward nonreacting shock or rarefaction wave, FW.

Given initial value (4.6), for $ab > 0$ suitably small, Corollary 3.5 guarantees the existence of shock profiles connecting (v_-, λ_-) to some $(v^*, \lambda^* = 1)$ with the speed

$$c_1 = \sqrt{-\frac{p^* - p_-}{v^* - v_-}} > 0.$$

Assume this shock profile is stable. To see that a wave pattern in Figure 1.2(b) is present in solutions of Riemann problems of (1.4), we choose $v_+ > v^*$ and such that the slope of the chord connecting $(v^*, p(v^*, 1))$ and (v_+, p_+) is larger than c_1^2; see Figure 4.2. Choose $u_\pm$ to satisfy the Rankine–Hugoniot condition

$$u_+ - u_- = -c_1(v^* - v_-) - c_2(v_+ - v^*);$$

then the Riemann problem (4.3) has a solution depicted in Figure 4.3. The pressure pattern of the solution is the same as depicted in Figure 1.2(b) for any fixed time.

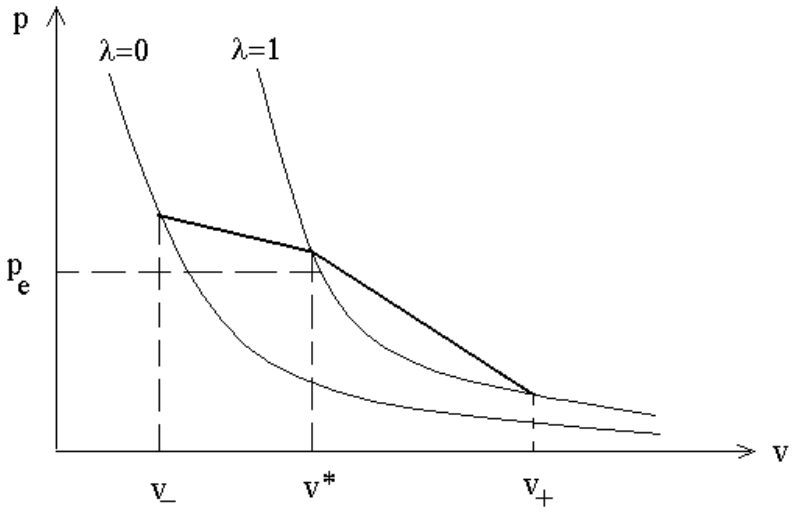

FIG. 4.2.

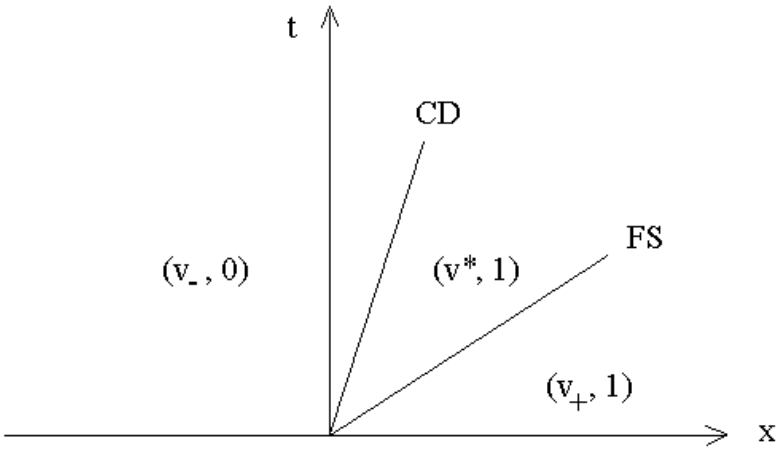

FIG. 4.3.

This solution consists of a nonreacting gas dynamic shock, FS, followed by a slower moving liquefaction shock, CD. The wave pattern of this solution is the same as Figure 1.2(b). One may notice that in Figure 1.2(b), it is mostly a mixture of liquid and vapor after the phase boundary. This is because when vapor condenses to liquid as it passes through the condensation discontinuity, latent heat is released which causes temperature to rise. This in turn raises the equilibrium pressure $p_e(T)$ which will stop the condensation and thus the condensation is partial and a mixture of liquid and vapor is created. The above solution of the Riemann problem is for the isothermal case which excludes the mechanism related to temperature change and hence we get the complete liquefaction shock.

The above example shows that solutions of (1.4) can exhibit the wave pattern depicted in Figure 1.2(b). Now we consider the possibility of the quantitative agreement of such a Riemann solver and the actual experimental data in order to assess

TABLE 4.1

M_0	p^* (bars)	p_1 (bars)	p^*_{exp}	$p_{1,exp}$	split?
1.81	3.646	3.835	3.60	3.80	Y
2.07	4.774	4.999	4.70	5.00	Y
2.13	5.056	5.267	5.00	5.10	Y
2.21	5.444	5.684	5.30	5.70	Y
2.44	6.640	6.896	6.50	7.10	N
2.48	6.860	7.118	6.85	7.60	N
2.72	8.258	8.519	7.85	8.85	N
2.81	8.813	9.075	8.85	10.48	N

the adequacy of the model (2.8), the "complete" version of (1.4). To fix ideas, we consider only experiments shown in Figure 1.2(b) since it is the one with most data available from [Gu, TCK, TCMKS]. Large differences between the calculation based on (2.8) and the experimental data can arise mostly for the following two reasons: (1) the system (2.8) is inadequate or (2) the state functions such as $p(v, \lambda)$ and parameters $\mu, \gamma, \epsilon, \alpha, \beta$, etc., are inaccurate. We see that once we know the solution is of the two-wave structure depicted in Figure 1.2(b), then the pressure p_0, p^*, and p_1 of the solution (see Figure 4.3) is completely determined by the Rankin–Hugoniot jump conditions. Rankin–Hugoniot conditions, stating the conservation of mass, momentum, and energy across shocks, depend only on state functions. Thus, if both the solution of (2.8) and the experiment with the same initial data show the two-wave structure depicted in Figure 1.2(b), then inaccuracy can arise only from reason (2). This indicates the possibility of quantitative accuracy of (2.8) by using more accurate state functions and parameters. Table 4.1 is Table 7.3 of [Gu] showing the calculated pressure p^* and p_1 from Rankin–Hugoniot conditions with Hobbs pressure function [Hobbs] with 64 terms, and with the corresponding pressure data observed in experiments. The fluid used in experiments is 2,2,4-trymethylpentane (iso-octan, C_8H_{18}). In the table, the pressure and temperature upstream are $p_0 = 1.1$ *bars* and $T_0 = 110^oC$; the Mach number of incident shock is M_0; subscript exp means the data are from actual experiments, while all other data are computed.

From the above reasoning, we see that difference between the calculation based on (2.8) and experiments due to reason (1) only occurs when the solution of (2.8) does not show the two-wave structure consisting of three almost constant pieces while the experimental data do. We claim that the difference caused by this reason is no more than $O(1)|p_\beta - p_e|$ under the assumption that $p_1(v.T, \lambda)$ and $p_1(v.T, \lambda)$ are convex in v, where p_β is the pressure at the vapor spinodal limit. Indeed, under the convexity assumption on p_1 and p_2 with respect to v, an admissible solution of the Riemann problem with $p_- < p_e > p_+$ and $\lambda_- = 0 < \lambda_+ = 1$, modeling the incident liquefaction shock propagating into stable vapor, consists of a backward nonreacting shock or rarefaction wave, a forward phase boundary, and a faster running forward nonreacting shock, as shown in Figure 4.1(b). Since the pressure p^* and actual pressure p_{exp} are in the range $p_e \le p^* \le p_\beta$ and the Rankin–Hugoniot jump conditions depend on p^* continuously, the errors in pressure data $|p_* - p_1|$ and $|p_{exp} - p^*|$ are of the order $O(1)|p_\beta - p_e|$. The same is true for all other quantities on two sides of the forerunning nonreacting shock and the trailing condensation discontinuity decided by Rankin–Hugoniot conditions. Of course, the above estimates are very rough. More detailed estimates and computations are left for future research.

Example 4.2. In this example, we intend to simulate Figure 1.2(a) where the piston is withdrawn, causing depressurization to induce evaporation. Let initial data

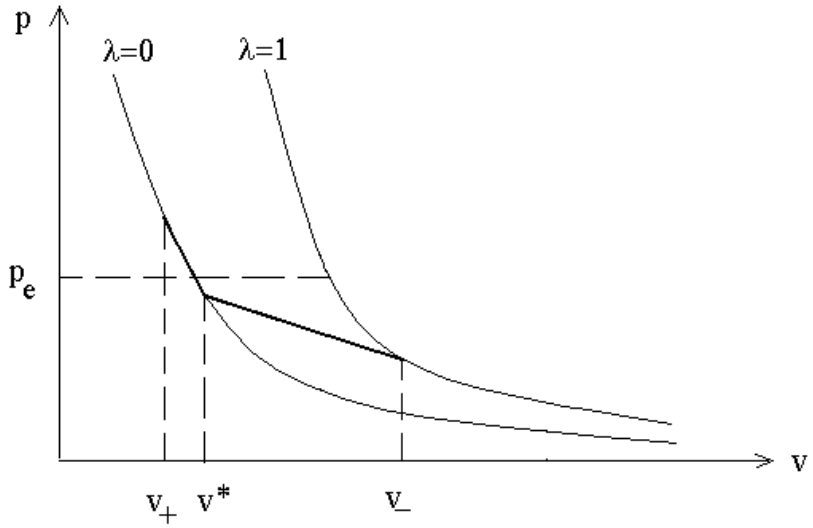

FIG. 4.4.

be

$$(u, v, \lambda)(x, 0) = \begin{cases} (u_- < 0, v_-, \lambda_- = 1) & \text{if } x < 0, \\ (u_+ = 0, v_+, \lambda_+ = 0) & \text{if } x > 0 \end{cases} \tag{4.11}$$

with $v_- > v_+$ and $p(v_+, \lambda_+) > p_e > p(v_-, \lambda_-)$.

In these initial data, the fluid is stable liquid at rest for $x > 0$ and stable vapor moving to the left for $x < 0$. Let v_- be such that there is an admissible shock that connects $(v_-, \lambda_- = 1)$ to $(v^*, \lambda^* = 0)$ with speed $c_1 > 0$ and $p^* < p_e$ and hence $v^* > v_+$; see Figure 4.4.

There is a nonreacting smooth rarefaction wave connecting v^* to v_+. Suppose $u_\pm$ are chosen to satisfy

$$u_+ - u_- = -c_1(v^* - v_-) + \int_{v^*}^{v_+} \sqrt{-p'(v, 0)}dv.$$

Then the solution of Riemann problem (4.3) with such Riemann initial data consists of a forward rarefaction wave FW and a slower forward evaporation discontinuity ES, as shown in Figure 4.5. The structure of the solution is the same as observed in experiments on retrograde fluids depicted in Figure 1.2(a).

Example 4.3. The first part of phenomenon (c) in section 1 states that withdrawing the piston from an equilibrium mixture of vapor and liquid creates a rarefaction shock. This kind of shock data are $\lambda_- = 1$, $\lambda_+ \in (0, 1)$, $p_- < p_e$, and $p_+ = p_e$. System (1.4) has such shocks as solutions since the existence of these rarefaction shocks is guaranteed by Theorem 3.4 and Corollary 3.5.

The second part of phenomenon (c) says that given a rarefaction initial data, where particles of the fluid are flowing away from each other, the system will sharpen up to form a (rarefaction) evaporation shock. This phenomenon is worth our attention since in classical shock theory of gas dynamics, rarefaction initial data lead to smooth rarefaction wave, not shocks.

Since the Riemann problem is not suitable for studying sharpening up of the solution, we shall numerically verify that this phenomenon is also present in system (1.4) in Eulerian coordinates in this example.

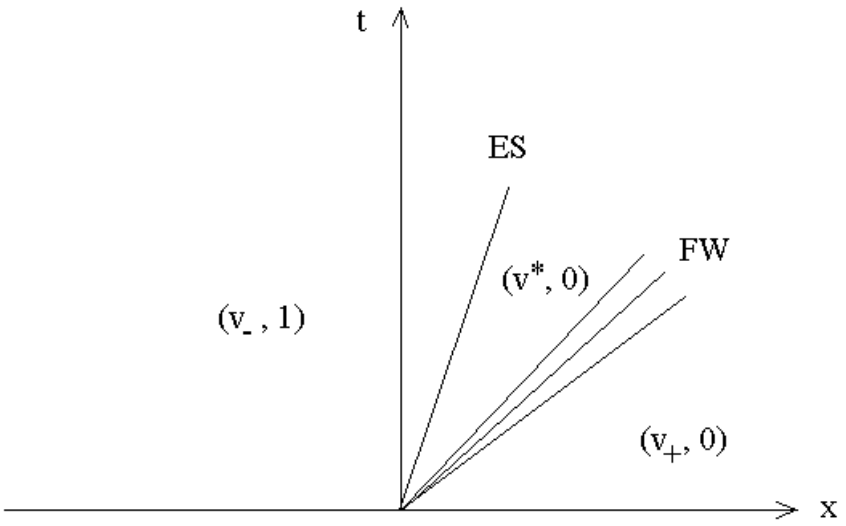

FIG. 4.5.

First we nondimensionalize the variables with respect to the critical state ρ_c, p_c and a typical length L, such as the diameter of the tube, as follows: $\rho = \bar{\rho}/\rho_c$, $m = \rho u = \bar{m}/(\rho_c p_c)^{1/2}$, $p = \bar{p}/p_c$, $T = \bar{T}/T_c$, $t = \bar{t}(p_c/\rho_c)^{1/2}/L$, and $x = \bar{x}/L$, where variables with bars denote variables with dimensions and those without bars are dimension-free variables. The standard van der Waals pressure function p for the above dimension-free variables is

$$h(\rho) = \frac{8T\rho}{3-\rho} - 3\rho^2. \tag{4.12}$$

In our computation, we take the temperature to be $T = 7.5/8$. Equilibrium pressure $p_e(T)$ can be computed from (4.12) by the Maxwell equal area rule. The pressure functions p_1 and p_2 used in the computation are

$$p_1(\rho) = \begin{cases} h(\rho) & \text{if } \rho \le \alpha, \\ h\left(\frac{\beta-3}{3-\alpha}(3-\rho)+3\right) + h(\alpha) - h(\beta) & \text{if } \rho > \alpha \end{cases}$$

and

$$p_2(\rho) = \begin{cases} h(\rho) & \text{if } \rho \ge \beta, \\ \frac{h(\beta)}{h(\alpha)} h\left(\frac{\alpha}{\beta}\rho\right) & \text{if } \rho < \beta. \end{cases}$$

The reaction rate function w_1 is taken as

(4.13)

$$\begin{aligned} w_1 =& \frac{p_{eq}-p}{\gamma p_{eq}} \lambda(1-\lambda)\rho \\ &+ \chi(0 \le \lambda \le 1)\frac{p_{eq}-p}{p_{eq}}\rho\left(c_1\chi(p<p_\beta) + c_2\chi(p>p_\alpha) + c_3 \exp\left(-\frac{c_4 p_{eq}^2}{(p-p_{eq})^2}\right)\right), \end{aligned}$$

where γ is the typical reaction time. The parameters in (1.4) used in the computations are $\epsilon = 0$, $\gamma = 0.005$, $\mu = 2\gamma/5$, $c_1 = c_2 = 1/\gamma$ $c_3 = 1$, and $c_4 = 0.1$. The grid steps are $\Delta x = 0.01$ and $\Delta t = 0.002$.

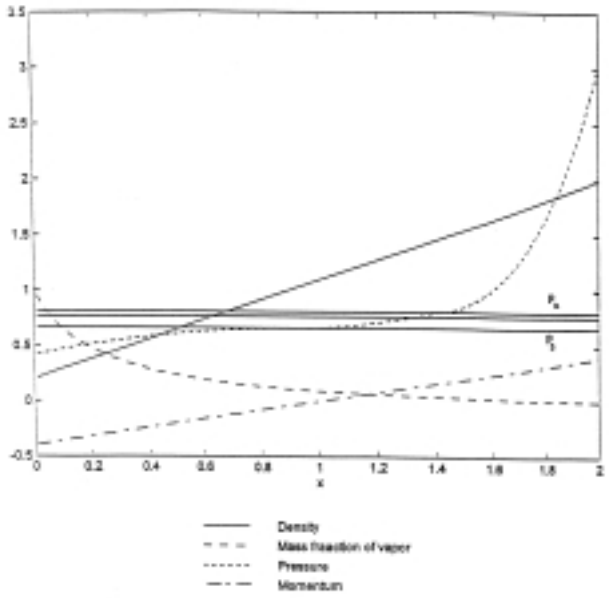

FIG. 4.6. *Initial data for Example* 4.3. *The fluid is stable vapor at* $x = 0$ *and stable liquid at* $x = 2$ *and smoothly varying in between. The three horizontal lines are, from high to low, the upper spinodal limit pressure* $p(v = \beta, \lambda = 1)$*, the equilibrium pressure* p_e*, and liquid spinodal limit pressure* $p(\alpha, \lambda = 0)$*. Thus, initial data is rarefying in the sense that the fluid on the left flows to the left, as indicated by the negative momentum, while that on the right flows to the right.*

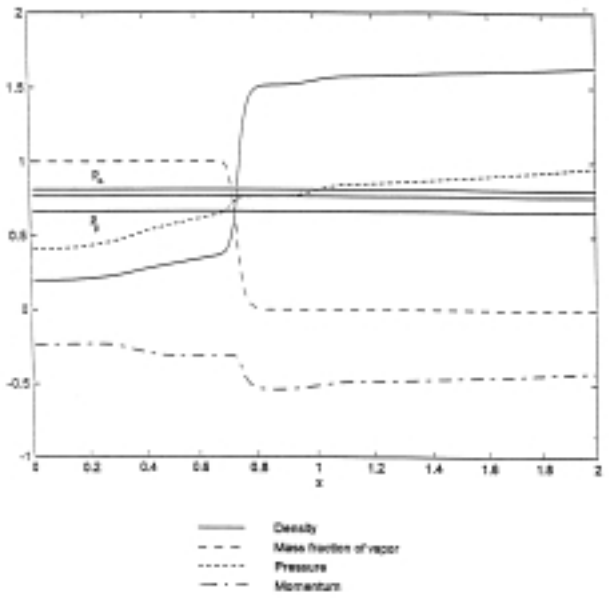

FIG. 4.7. *At time* $t = 1.332$*, the solution sharpens up from the smooth initial data shown in Figure* 4.6(a) *to a rarefaction shock.*

The numerical method we used is as follows. We discretize the diffusion terms by central difference. Since we expect that the speed of the phase boundary is sensitive to diffusion terms as indicated by Theorem 1.2, the numerical viscosity should be made at least one order smaller than the diffusion terms. For this reason, we used the third-order WENO method [JS] to discretize the left-hand side of (1.4). Iteration scheme in time is the third-order Runge–Kutta method, also from [JS].

The initial data are shown in Figure 4.6, where the fluid is stable vapor at $x = 0$ and stable liquid at $x = 2$ and smoothly varying in between. The three horizontal lines in Figures 4.6 and 4.7 are, from high to low, the upper spinodal limit pressure $p(v = \beta, \lambda = 1)$, the equilibrium pressure p_e, and liquid spinodal limit pressure $p(\alpha, \lambda = 0)$. The fluid on the left flows to the left, as indicated by the negative momentum, while that on the right flows to the right. Thus, it is a rarefaction initial data. As shown in Figure 4.6(a), the initial data are quite smooth. Figure 4.6(b) shows that at time $t = 1.332$, the solution sharpens up to a rarefaction shock. Thus, system (1.4) also exhibits the wave pattern (c).

REFERENCES

[Ba] D. Bauschdorff, *Carrier gas effects on homogeneous nucleation of water vapor in a shock tube*, Phys. Fluids, 18 (1975), pp. 529–535.

[FD] W. Fickett and W. C. Davis, *Detonation*, University of California Press, Berkeley, CA, 1979.

[Fan1] H. Fan, *One-phase Riemann problem and wave interactions in systems of conservation laws of mixed type*, SIAM J. Math. Anal., 24 (1993), pp. 840–865.

[Fan2] H. Fan, *Traveling waves, Riemann problems and computations of a model of the dynamics of liquid/vapor phase transitions*, J. Differential Equations, 150 (1998), pp. 385–437.

[Gu] S. C. Gulen, *A Study of Shock Splitting and Liquefaction Shocks in Fast Phase Changes in Retrograde Fluids*, Ph.D. dissertation, Rensselaer Polytechnic Institute, Troy, NY, 1992.

[GTC] S. C. Gulen, P. A. Thompson, and H. J. Cho, *An experimental study of reflected liquefaction shock waves with near critical downstream states in a test fluid of large molar heat capacity*, J. Fluid Mech., 277 (1994), pp. 163–196.

[Hobbs] D. E. Hobbs, *A Virial Equation of State Utilizing the Corresponding State Principle*, Ph.D. thesis, Rensselaer Polytechnic Institute, Troy, NY, 1983.

[Hs] L. Hsiao, *Uniqueness of admissible solutions of Riemann problem of systems of conservation laws of mixed type*, J. Differential Equations, 86 (1990), pp. 197–233.

[JS] G.-S. Jiang and C. W. Shu, *Efficient implementation of weighted ENO schemes*, J. Comput. Phys., 1261 (1996), pp. 202–228.

[KG] S. Kotake and I. I. Glass, *Flows with nucleation and condensation*, Progr. Aerospace Sci., 19 (1981), pp. 129–196.

[MP] R. Menikoff and B. J. Plohr, *The Riemann problem for fluid flow of real materials*, Rev. Modern Phys., 61 (1989), pp. 75–130.

[Ox] D. W. Oxtoby, *Homogeneous nucleation: Theory and experiment*, J. Phys. Condens. Matter, 4 (1992), pp. 7627–7650.

[RFF] R. L. Rabie, G. R. Fowles, and W. Fickett, *The polymorphic detonation*, Phys. Fluids, 22 (1979), pp. 422–435.

[Sh] M. Shearer, *Nonuniqueness of admissible solutions of Riemann initial value problem for a system of conservation laws of mixed type*, Arch. Rational Mech. Anal., 93 (1986), pp. 45–59.

[SG] J. P. Sisilian and I. I. Glass, *Condensation of water vapor in rarefaction waves:* I. *Homogeneous nucleation*, AIAA J., 14 (1976), pp. 1731–1737.

[Sl] M. Slemrod, *Admissibility criterion for propagating phase boundaries in a van der Waals fluid*, Arch. Rational Mech. Anal., 81 (1983), pp. 301–315.

[Sp] G. S. Springer, *Homogeneous nucleation*, Adv. in Heat Transfer, 14 (1978), pp. 281–345.

[SX] A. Szepessy and Zhouping Xin, *Nonlinear stability of viscous shock waves*, Arch. Rational Mech. Anal., 122 (1993), pp. 53–103.

[TCK] P. A. Thompson, G. C. Carofano, and Y.-G. Kim, *Shock waves and phase changes in a large-heat-capacity fluid emerging from a tube*, J. Fluid Mech., 166 (1986), pp. 57–92.

[TCMKS] P. A. Thompson, H. Chaves, G. E. A. Meier, Y.-G. Kim, and H.-D. Speckmann, *Wave splitting in a fluid of large heat capacity*, J. Fluid Mech., 185 (1987), pp. 385–414.

[VVV] A. I. Volpert, V. A. Volpert, and V. Volpert, *Traveling Wave Solutions of Parabolic Systems*, Transl. Math. Monogr. 140, AMS, Providence, RI, 1994.

[Wa] G. B. Wallis, *One-Dimensional Two Phase Flow*, McGraw–Hill, New York, 1969.

[WLe] P. P. Wegener and C. F. Lee, *Condensation by homogeneous nucleation of H_2O, C_6H_6, CCl_4 and CCl_3F in a shock tube*, J. Aerosol. Sci., 14 (1983), pp. 29–37.

[WLu] P. P. Wegener and G. Lundquist, *Condensation of water vapor in the shock tube below* 150 *K,* J. Appl. Phys., 22 (1951), p. 233.

[Wu] B. J. C. Wu, *Analysis of condensation in the centered expansion wave in a shock tube*, in Condensation in High Speed Flows, A. A. Pouring, ed., ASME, New York, 1977, pp. 73–82.

[WW] P. P. Wegener and B. C. J. Wu, *Gas dynamics and homogeneous nucleation*, in Nucleation Phenomena, A. C. Zettlemoyer, ed., Elsevier, New York, 1977, pp. 325–417.

[X] Z. P. Xin, *Asymptotic stability of rarefaction waves for* 2×2 *viscous hyperbolic conservation laws*, J. Differential Equations, 72 (1988), pp. 45–77.

[ZBLM] Ya. B. Zeldovich, G. I. Barenblatt, V. B. Librovich, and G. M. Makhviladze, *The Mathematical Theory of Combustion and Explosions*, Consultants Bureau, New York, 1985, p. 4.